

8-2019

Enhancing Transport in Classical and Quantum Systems Using Non-Hermiticity

Fatemeh Mostafavi
The University of Texas Rio Grande Valley

Follow this and additional works at: <https://scholarworks.utrgv.edu/etd>



Part of the [Physics Commons](#)

Recommended Citation

Mostafavi, Fatemeh, "Enhancing Transport in Classical and Quantum Systems Using Non-Hermiticity" (2019). *Theses and Dissertations*. 552.
<https://scholarworks.utrgv.edu/etd/552>

This Thesis is brought to you for free and open access by ScholarWorks @ UTRGV. It has been accepted for inclusion in Theses and Dissertations by an authorized administrator of ScholarWorks @ UTRGV. For more information, please contact justin.white@utrgv.edu, william.flores01@utrgv.edu.

ENHANCING TRANSPORT IN CLASSICAL AND QUANTUM SYSTEMS
USING NON HERMITICITY

A Thesis

by

FATEMEH MOSTAFAVI

Submitted to the Graduate College of
The University of Texas Rio Grande Valley
In partial fulfillment of the requirements for the degree of

MASTER OF SCIENCE

AUGUST 2019

Major Subject: Physics

ENHANCING TRANSPORT IN CLASSICAL AND QUANTUM SYSTEMS
USING NON HERMITICITY

A Thesis
by
FATEMEH MOSTAFAVI

COMMITTEE MEMBERS

Dr. Hamidreza Ramezani
Chair of Committee

Dr. Soumya D Mohanty
Committee Member

Dr. Volker Quetschke
Committee Member

Dr. Cem Yuce
Committee Member

AUGUST 2019

Copyright 2019 FATEMEH MOSTAFAVI

All Rights Reserved

ABSTRACT

MOSTAFAVI FATEMEH, Enhancing Transport in Classical and Quantum systems Using Non Hermiticity. Master of Science (MS), AUGUST, 2019, 58 pp., 26 figures, 74 titles.

Non-Hermiticity, provides a flexible platform to have control over the dynamics of the system. This thesis will present a theoretical investigation toward population inversion in quantum mechanical systems and the topological zero-mode in a non-Hermitian optical lattice. Firstly, an adiabatic process is a common approach to describe the evolution of a system under slow successive changes. However, in practice, finding a realistic adiabatic process is almost impossible due to the existence of some non-adiabatic parameters. While many approaches have been proposed to cancel the non-adiabaticity contribution, all provide the shortcut with cost of imposing more energy. We propose a new class of Hamiltonians that provides an alternative dynamical approach, takes the system to the desired eigenstate, rather than forcing it to end in a specific state. Meanwhile, it can reduce the cost and remove the existing complications in other shortcuts. Secondly, we study the topologically protected state. Generally, a bound state is expected when we break periodicity. However, not only all of the bound state does not maintain zero-energy but also, they are vulnerable to local perturbation, while the topologically bound state provides protection against disorder. Nonetheless, the topological localized state vanishes as the defect interface maintains the same topology as its neighbor. We propose a mechanism, where control over the dissipation rather than the transition between different phases or topological order creates a robust zero mode.

DEDICATION

To my dearest sister, my parents and family for their endless love, support and encouragement.

ACKNOWLEDGMENTS

First and foremost, I would like to thank my parents for their love and support throughout my life. My sister and little brother for their encouragement in my crisis moments. Thank you so much.

I would also like to sincerely thank my advisor Dr. Ramezani, for his guidance throughout my research and beyond.

Next, I want to thank the faculty of the UTRGV physics department, specially professor Mukherjee for her support during my two-year presence at UTRGV.

TABLE OF CONTENTS

	Page
ABSTRACT	iii
DEDICATION	iv
ACKNOWLEDGMENTS	v
TABLE OF CONTENTS	vi
LIST OF FIGURES	viii
CHAPTER I. INTRODUCTION	1
1.1 Geometric Phase :	1
1.2 Adiabatic Theorem and Berry Phase :	4
1.3 Topology and Berry Phase :	5
1.4 Berry Phase and Winding Number :	7
CHAPTER II. QUANTUM EVOLUTION VIA DIABATIC PROCESS	11
2.1 General overview on Adiabatic Evolution	12
2.2 Alternative Approaches to Adiabatic Population Transfer	13
2.3 Landau-Zener Formalism, The Spirit Of The Population Transfer	14
2.4 Non-Hermitian Shortcut to Adiabaticity	18
2.5 Dynamical Approach to Low-Cost Shortcut to Adiabaticity(DASA)	21
2.6 Extension To Higher Dimension	28
2.7 DASA Vs traditional Shortcut to Adiabaticity	34
2.8 Experimental Setups	35
2.9 Summary	37
CHAPTER III. TOPOLOGICAL LOCALIZED STATE AT WILL	38
3.1 Non-Hermitian PT Symmetric System	39
3.2 Localized Mid-gap State in Non-Hermitian Lattice	41
3.3 Topological invariant in the Non-Hermitian System	43
3.4 Robust Localized Zero-Mode State Via Phase Transition in Non-Hermitian PT Symmetric Lattice	44

3.5	Zero-Mode Protected State at Will in PT Symmetric Lattice	47
3.6	Robustness of the zero mode	51
3.7	Summary	52
	REFERENCES	53
	BIOGRAPHICAL SKETCH	58

LIST OF FIGURES

	Page
Figure 1.1: The holonomy or adiabatic itinerary transportation of a pendulum on the surface of the sphere.	3
Figure 1.2: Sketch of dimer lattice structure. Two different sublattices distinguished by A and B per unit cell in which the n numerate the unit cell through the lattice.	6
Figure 1.3: Real part of dispersion, $Re E(q)$, of the extended states for the biatomic lattice where the couplings are assumed either $k = 1$ and $c = 0.5$ or $k = 0.5$ and $c = 1$	7
Figure 1.4: Sketch of eigenenergy $ReE(q)$ of the finite chain of dimer $N = 16$, represented, left figure, trivial band where all the modes are placed in the continuum with $k = 1$ and $c = 0.5$, and right figure, the non-trivial band making two localized eigenstate corresponding to zero energy $k = 0.5$ and $c = 1$	8
Figure 1.5: Topological characterization of the Hermitian system. plot shows the trace of the $H(k)$ in xy plane. Where the red circle represent the non-trivial band structure with $c = 1$ and $k = 0.5$, the blue circle represent the trivial band where $c = 0.5$ and $k = 1$	9
Figure 2.1: Left figure shows the ground state of a particle in quadratic potential $U = \frac{1}{2}m\omega^2x^2$. While, the right figure represent the first four stationary state of the particle in the $U = \frac{1}{2}m\frac{\omega^2}{2}x^2$ when the potential changes so rapidly, caused the final state be a superposition state.	14
Figure 2.2: Left figure: Bare energy corresponding to the states $ 0\rangle$ and $ 1\rangle$ crossing through the time in Landau- Zener Model. Right figure: Bare energy corresponding to the states $ 0\rangle$ and $ 1\rangle$ in the Landau- Zener Model adiabatic transition, while the coupling between the states avoids crossing.	16
Figure 2.3: Time evolution of population transfer in the Landau- Zener Model for the two-level system. (left figure) shows the ground states flips from state $ 0\rangle$ to $ 1\rangle$ under the adiabatic passage. Right figure represents non-level crossing evolution of states under the non-adiabatic passage.	18
Figure 2.4: Time evolution of population transfer in the Landau- Zener model for the two-level system, while we speed up the process $\epsilon = 5$ and increase the coupling or interaction strength of the two state to $k = 10$	19

Figure 2.5: Evolution of population and transition between the ground state in the non-Hermitian LZ model (left plot). external field or γ function with respect to time and for different values for parameter ε which defines the speed of the diabatic process.[65]	20
Figure 2.6: Real (left column) and imaginary (right column) part of the $g_{1,2,3}$ as a function of the γ_2 for $\Delta\omega = 1, 2, 3, 4$. All region make the g as the real function are acceptable. fore instance, we do not have restriction on choosing the correct value fom g_3 , as it is a real function. As the other functions are generally complex, the accepted values are the one make the imaginary part equal to zero. Therefore, one eigenvalues of Hamiltonian in Equation.(2.18) becomes absolutely real and the other one becomes complex. Figure is taken from [71]	25
Figure 2.7: Amplitude probability of the bare states $(0, 1)^T$ and $(1, 0)^T$ as a function of time (in the unit of coupling) using the Hamiltonian $\mathcal{H}_{2\times 2}(t)$. Figure is taken from [71]	28
Figure 2.8: Dynamics of a three-level Landau-Zener model (amplitude probability of the bare states $(0, 0, 1)^T$ and $(0, 1, 0)^T$, and $(1, 0, 0)^T$ as a function of time in the unit of outer coupling) associated with the Hamiltonian in Equation.(2.29) for (a) $\kappa = 0$, $\mathcal{E}_2 = 0$, and $\varepsilon = 0.5$, (b) $\kappa = 0$, $\mathcal{E}_2 = 15$, and $\varepsilon = 0.5$, (c) $\kappa = 0$, $\mathcal{E}_2 = 15$, and $\varepsilon = 0.05$, (d) $\kappa = 0.5$, $\mathcal{E}_2 = 15$, and $\varepsilon = 0.5$. We observe that in the absence of strong coupling between the third level and the first level when the on-site potential of the middle level becomes large one needs to make the process much slower in comparison to the two-level system in order to have adiabatic process. Specifically, while for $\varepsilon = 0.5$ one gets a complete population transfer in the two-level system (Figure.2.7 a), as depicted in Figure.(2.8b) for a three-level system with the same ε and $\mathcal{E}_2 = 15$ there wont be any population transfer to the ground state if the first and third level are not directly coupled, namely $\kappa = 0$. Figure is taken from [71]	30
Figure 2.9: Amplitude probability of the bare states $(0, 0, 1)^T$, $(0, 1, 0)^T$, and $(1, 0, 0)^T$ as a function of time using the Hamiltonian in Equation.(2.35) using the same gain and loss parameters that are obtained for the two-level system, namely $\mathcal{H}_{2\times 2}$ in the main text. We observe that, in a very short time a complete population transfer occurs. Figure is taken from [71]	33

- Figure 2.10: Upper figure, schematic of the proposed photonic structure to realize the dynamical approach to shortcut to adiabaticity. Our proposed structure composed of two waveguides. Each waveguide has two segments. The left waveguide in the first segment between $z = 0, z_1$ (indicated by the red color) has index of refraction $n_1^l - i\gamma_1^l$ while the right waveguide in the first segment has loss with refractive index $n_1^r - i\gamma_1^r$. In the second segment the left and right waveguides have refractive index $n_2^l + i\gamma_2^l$ and $n_2^r + i\gamma_2^r$ respectively. One can achieve complete population transfer in no time in terms of the electric fields if the values of $\gamma_{1,2}^l$ are chosen according to the g -functions in Equation.(2.25) and the real part of the refractive indexes are replaced by $\omega_{1,2}$. The bottom figure, Electronic implementation of dynamical approach to shortcut to adiabaticity. The coils are inductively coupled with V_1 and V_2 providing access to the system variables. The switch S asserts the initial condition. A resistor provides the damping (green side) while a negative resistance gain element (red side) is implemented by feedback from an LM356 voltage doubling amplifier. Current flows in the direction of the arrows proportional to the respective voltages V_1 and V_2 . Figures are taken from [71] 36
- Figure 3.1: Sketch of Non-Hermitian chain of dimers structure. Two different sublattices distinguished by A represents the gain waveguide/resonator and B represents lossy waveguide/resonator, per unit cell, with $\pm i\gamma$ as the imaginary part of the on-site potential. 39
- Figure 3.2: Sketch of dispersion relation of the complex SSH model. Left Figure, $\text{Re } E(q)$ and right figure dispersion $\text{Im } E(q)$ of the extended states for the biatomic lattice for various values of γ as the non-Hermitian part of the Hamiltonian and when the coupling $k = 0.5$ and $c = 1.5$. The dispersion relation are gapped when $\gamma < \gamma_c$ and the whole structure is in the exact phase of the PT system where the bands are totally real. The band gap closes at the phase transition point called exceptional point at $q = \pm\pi$. Then after, when the γ exceed the critical value. 41
- Figure 3.3: (a)Two coupled complex SSH chain with alternating bond k and c and alternating on-site potential $\pm i\gamma$ presenting two distinct topological configurations, result in having the defect state at the interface of two structures.(Bottom figure), As long as the on-site potential $\gamma < \gamma_c = |k - c|$, the exponentially localized state confined in the A sublattices when $k = 1$ and $c = 0.5$ 43
- Figure 3.4: Schematic of an interface realized by two dissipative SSH semi-lattice with uniform coupling relation $t_A > t_B$ through the whole structure. Although the interface coupling has the same topological order as its neighbours, variation of gain/loss caused phase transition. Sites A have lower decay rates δ or 0 and sites B are associated with higher rates Δ or σ . Figure is taken from [25]. 45

- Figure 3.5: Energy diagram of the interface states for $\frac{t_A}{t_B} = 2.5$ and $\sigma = 2.5t_B$, and for the right semi-array in the unbroken PT phase (phase I: $\delta = 2.5t_B$). As $\frac{\Delta}{t_B}$ increases, five distinct regions can be defined: Region I, no interface state exist; Region II, there are two interface modes with opposite real part of energy; Region III, two zero-energy modes exist with different decay rates; Region IV, one of the two zero-energy modes becomes dominant in the system; Region V. The value of $\frac{\Delta}{t_B}$, separates regions III and IV is the threshold value $\frac{\Delta_{th}}{t_B}$ required to observe a dominant zero-energy mode in the dynamics. The insets show a few distributions of mode amplitudes of interface states at a few values of $\frac{\Delta}{t_B}$. Figure is taken from [25]. 46
- Figure 3.6: (a) The schematic of array of waveguides maintain zero-mode state at the interface of PT broken and un-broken phase of semi-lattices. (b) Schematic of the perturb structure where the interface waveguide is shifted by a distance D from its original place. Therefore the disorder applied to the interface coupling. (c) Evolution of eigen-spectrum with respect to the shift of the interface waveguide. The interface state robustly resides at zero energy apart from the extended states. (d-e) Intensity of the the localized state with zero-energy correspond to different shift at the interface waveguide. Figure is taken from [25]. 47
- Figure 3.7: Sketch of dispersion, $\text{Re } E(q)$, of the extended states for the biatomic lattice where $\gamma = 0$ and the gap is open. On the other hand, $\gamma = 0.5$ reduced the effective coupling. Therefore, the gap is closed when $k = 0.5$ and $c = 1$ 48
- Figure 3.8: The mode amplitude of the localized state at the interface of two non-trivial structure. Left figure, when $\gamma = 0$ and localized state has real value eigenmode due to hermiticity of the structure. Right figure, when $\gamma = 0.041$ applied to the whole structure represents the PT symmetric lattice. 49
- Figure 3.9: As the non-Hermiticity increases from $\gamma = 0$ toward the critical value $\gamma = 0.041$, the real part of the defect mode decreases while imaginary part grows, till the mode falls into its complete broken phase and energy pins to zero. 50
- Figure 3.10: Topological localized state at the interface of two semi-infinite non-trivial lattices when $d = 0.4$ and $\gamma = 0.41$ applied to the edge sites, Left plot. Amplitude of the localized state (Blue state) emerges in the PT structure, compared with the decoupled state appear as non-Hermiticity applied to the edge sublattice, Red mode profile in the right plot. 51
- Figure 3.11: Robustness of the bound state mode at the presence of disorder with different strength. The plot shows that the defect mode when it falls into its broken phase, still pines to zero and is protected against local change applied to the structure. . . 52

CHAPTER I

INTRODUCTION

1.1 Geometric Phase :

Geometric phase, introduced by Berry, back in 1984 [1], manifests itself in many different areas of physics from Foucault pendulum, polarized light, spin system to adiabatic and non-adiabatic theorem, in addition to topology of the system [2]. In the present chapter, we review the geometric or Berry phase and its origin. Among lots of applications, we have discuss the two topics related to the Berry phase. In particular, I will start with the review on the geometric phase, which interestingly is a kind of property of the space and structure that only depends on the geometry of the system therefore its effect can not be removed. It is also connected to the topology of the structure and naturally arises in the evolution of the classic or the quantum system through gradual variation occurs in the parameters of the space. Firstly, we investigate the idea of population transfer in the open quantum system through the non-adiabatic process that provides the same results as its adiabatic counterpart. Then, in the second part, we explore the topological robust state.

To introduce the Berry phase which is defined as the phase angle of the complex vector evolves through a path, lets look at a system with a time-independent Hamiltonian $H(r, p)$. Generally, the wavefunction of the quantum system could be considered as the complex vector and expand based on the the eigenstate, $|n\rangle$, of the Hamiltonian. Through the time evolution of the system, an initial state $|\psi_0\rangle = \sum c_n |n\rangle$ evolves into final state $|\psi_t\rangle = \sum e^{-\frac{i}{\hbar} H t} c_n |n\rangle$ at time t . In this case, the particle just acquires the dynamical phase while the probability of finding the particle in state remains unchanged. Now let's pay attention to another form of Hamiltonian, suppose the

system is time-dependent and the time evolution of the Hamiltonian governed by the time-dependent Schrödinger equation described by

$$i\hbar\partial_t|\psi_t\rangle = H(R(t))|\psi_t\rangle \quad (1.1)$$

in which the time dependency of the Hamiltonian recognize by the $R(t)$ that adiabatically vary through the time. According to the adiabatic theorem if a system with non-degenerate and discrete spectrum be prepared in one of its eigenstates and undergoes gradual evolution, then it would not be found in any other eigenstate of the system than the initial one [3, 4]. In 1984, Berry looked at the adiabatic theorem from another perspective and brought attention to a non-dynamical phase called the geometric phase. A very good example to clarify the geometric phase could be the evolution of the pendulum while we move it slowly on the surface of the sphere. Suppose, you have a pendulum and start to bring it from the north pole and move the pendulum down while keeping it in the same direction till you reach to one of the longitudinal lines parallel the equator, then move parallel to the equator till you make an angle φ with the origin and reach to the next meridian, next move it upward to the north pole, at this point although the pendulum returns to its original place, it has turned around an angle φ Figure(1.1). Keep in mind that during all the evolution you keep the pendulum in your hand as steady as possible. In other words no sudden changes applied to the oscillation. This phenomenon called holonomy [2, 5].

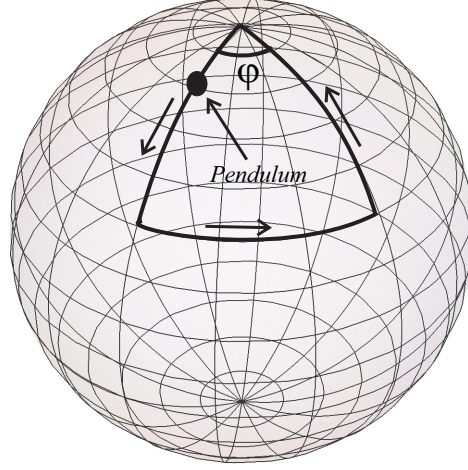


Figure 1.1: The holonomy or adiabatic itinerary transportation of a pendulum on the surface of the sphere.

This is a simple and classic example where the geometric phase arises in the system, transformed in the closed path. This concept also arises in the context of quantum mechanics when the Hamiltonian and consequently the wave function or an eigenstate of the time-dependent Hamiltonian, $H(t)$ acquires a geometric phase represents local changes in between two states when the state undergoes slow continuous cyclic evolutions, meaning, a particle starts from the eigenstates of the $H(0)$ and end up to the eigenstates of the $H(t)$ picking up a phase factor in addition to its dynamical phase[1, 2].

$$\psi(t) = e^{i\theta_n(t)} e^{i\gamma_n(t)} \psi_n(t) \quad (1.2)$$

where

$$\theta_n(t) \equiv -\frac{1}{\hbar} \int_0^t E_n(t') dt' \quad (1.3)$$

is dynamical phase and

$$\gamma_n(t) \equiv i \int_0^t \langle \psi_n(t') | \frac{d}{dt'} \psi_n(t') \rangle dt' \quad (1.4)$$

called geometric phase or Berry phase. The Equation.(1.4) can be written in the the form of

$$\gamma_n(t) = i \int_0^t \langle \psi_n(t', R) | \frac{d}{dR} \frac{dR}{dt'} \psi_n(t', R) \rangle dt' = i \int_{R_i}^{R_f} \langle \psi_n | \frac{d\psi_n}{dR} \rangle dR \quad (1.5)$$

where the $R \equiv R(t)$ are some parameters changing through the time. and if there are more than one parameter the Equation.(1.5) becomes,

$$\gamma_n(t) = i \int_{R_i}^{R_f} \langle \psi_n | \nabla_R \psi_n \rangle dR \quad (1.6)$$

in which the $i \langle \psi_n | \nabla_R \psi_n \rangle$ defines as Berry connection and the integral is taken in a closed path in the parameter space R. In the one dimension case which we deal with it through chapter 3 the Berry phase specifically called and replaced by Zak phase.

As stated above, we have divided this thesis into two major parts. Firstly, we explore the quantum state manipulation and look at the quantum population transfer in chapter 2. In chapter 3, we look into the topological properties of the system and controlling the topological characteristics of the structures by introducing an unexplored approach that has not been looked over. But, before delving into these areas, I would like to give a brief introduction about the main ideas which have been developed and how they have been structured in this thesis.

1.2 Adiabatic Theorem and Berry Phase :

In the previous section, It was sated how adiabatic process naturally leads to the emergence of the Berry phase. Quantum adiabatic theorem with its application in a wide variety of areas ranging from quantum field to adiabatic computation, plays an important role in today's life, specially, in one of its interesting and intrinsic consequences to prepare the quantum system and wave packet for a desired state. In the following chapter, we deal with quantum evolution and population transfer directly focus on steering the system for a specific configuration. As mentioned before, according to the adiabatic theorem, if a system prepared in the ground state, experiences gradual external changes in its parameters, it has enough time to adapt itself with

the new configuration of the system. Consequently satisfies the boundary condition and therefore, will remain in the instantaneous ground state of the Hamiltonian. However, practically providing the necessary and ideal condition of an adiabatic process is very hard, for example, one of the consequences of such a long process is that there always exist diabatic channels and noise in the system. Besides, it is not desired to make the process slow to satisfy the adiabatic condition. Now the question is that how one can make the process faster while ending up with the same result that adiabatic passage provides. In chapter 2 we address this issue.

1.3 Topology and Berry Phase :

The last chapter of this thesis is dedicated to topology, natural fundamental properties of an object, where I briefly review the topological structures. The topological characteristic is investigated in many different areas since it is robust against any kinds of gradual deformation unless the applied changes do not destroy the nature of the structure. This stable property of any structure do exist and result in remarkable characteristics even at the quantum level [6] with widespread application in material science, electronic engineering, computer science, quantum information [7, 8, 9, 10] and photonics [11, 12, 13, 14, 15, 16, 17, 18, 19, 20].

Our analytical and numerical calculation in this chapter are mainly focused on the one dimensional lattice. So, it's good to start with the description of the one-dimensional (1D) Su-Schrieffer-Heeger (SSH) model which describes a finite dimer lattice with first-neighbor couplings [21, 22]. This model is based on a one-dimensional (1D) array of dimer depicted in Figure (1.2) , consisting of two different sublattices A and B grouped in unit cell and each of them hosting a single state with the amplitudes ψ_n^A and φ_n^B in each of them respectively, which can be set up with an array of coupled resonators or waveguides. The coupling factor in a dimer (intra pair) is denoted by k , while the outer coupling (inter-pair) is denoted by c . It is good to mention that the coupling is tunable via changing the distance between the two resonators and in the case of $k \neq c$ caused dimerization. The tight-binding model equations for such lattice is

given by the Schrödinger like equation that describes the time evolution of the field or the dynamics of each electron or photon in each sublattices which gives us the allowance to know about the behavior of the wave function according to :

$$\begin{aligned} i\partial_t \psi_n^A &= k\phi_n^B + c\phi_{n-1}^B \\ i\partial_t \phi_n^B &= k\psi_n^A + c\psi_{n+1}^A \end{aligned} \quad (1.7)$$

therefore, the associated Hamiltonian using the Bloch theorem is given by,

$$H(q) = (c\cos(q) + k)\sigma_x + c\sin(q)\sigma_y \quad (1.8)$$

where q is the Bloch wave number and σ are the Pauli matrices. As the unit cell constructed from two sites, when we diagonalized the Hamiltonian the dispersion relation of the structure is made up of two bands given by

$$E(q) = \pm \sqrt{(c^2 + k^2 + 2ck\cos(q))} \quad (1.9)$$

Based on how dimerization occurs in the system, the band structure of the terminated chain would be different although the infinite band is exactly the same. So, when the intracoupling is stronger than the intercoupling couplings or vice vers, the gap opens and the two bands are separated symmetrically around $E = 0$ shown in Figure(1.3).

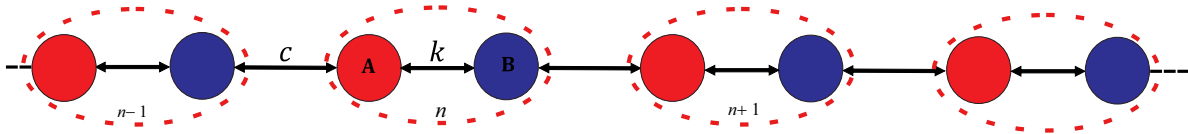


Figure 1.2: Sketch of dimer lattice structure. Two different sublattices distinguished by A and B per unit cell in which the n numerate the unit cell through the lattice.

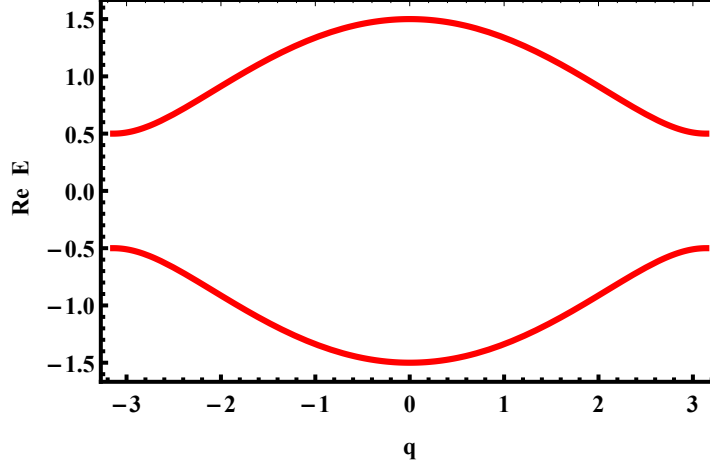


Figure 1.3: Real part of dispersion, $\text{Re } E(q)$, of the extended states for the biatomic lattice where the couplings are assumed either $k = 1$ and $c = 0.5$ or $k = 0.5$ and $c = 1$.

1.4 Berry Phase and Winding Number :

Now let's return to the topology of the structures. In particular, topological invariants called the Winding number which is defined by loop integral of the local gauge transformation over the Berry phases, in the $1D$ system, specifies the topological properties of the system. From this point of view, the structure is divided into two categories, either topologically trivial or non-trivial. The terms trivial and non-trivial refers to the presence or absence of the localized edge state with zero energy in the band structure. Based on two different configurations that is possible for dimerization which both of them resulted in the same band structure trivial or non-trivial band is accessible. Suppose the finite Hermitian system of the one-dimensional lattice described by the Equation.(1.8). As mentioned earlier, the Winding number defines by loop integral over the Berry phases which in the Hermitian system is exactly the Zak phase divided by π and calculated through [23]

$$W = \frac{1}{2\pi i} \oint dq \frac{d}{dq} \ln(h(q)) \quad (1.10)$$

where $h(q) = k + ce^{iq}$. The integral yields to $|W| = 0$ or 1 , when $k > c$ corresponding to the trivial band or $c > k$ for non-trivial case respectively. As an example, for the finite structure

controlled by the Hamiltonian in Equation.(1.8), for $N = 16$ and $c > k$ the band structure clearly shows two modes separated from the continuum represented the two localized modes Figure(1.4), while in the other case none of the modes is out of the continuum so there will not be any localized state .

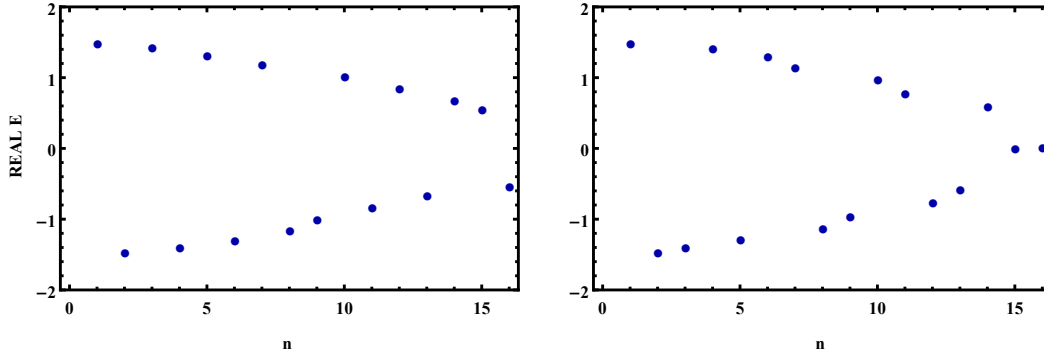


Figure 1.4: Sketch of eigenenergy $ReE(q)$ of the finite chain of dimmer $N = 16$, represented, left figure, trivial band where all the modes are placed in the continuum with $k = 1$ and $c = 0.5$, and right figure, the non-trivial band making two localized eigenstate corresponding to zero energy $k = 0.5$ and $c = 1$.

Moreover, two distinct topology are distinguishable by the trajectory of the eigenstates of the Hamiltonian shown in Figure(1.5) represent the trivial and non-trivial characteristic of the Hamiltonian. This trajectory is given by the internal structure of the stationary states and the components of the Hamiltonian in momentum space as

$$\sigma_x = c \cos(q) + k, \quad \sigma_y = -c \sin(q), \quad \sigma_z = 0 \quad (1.11)$$

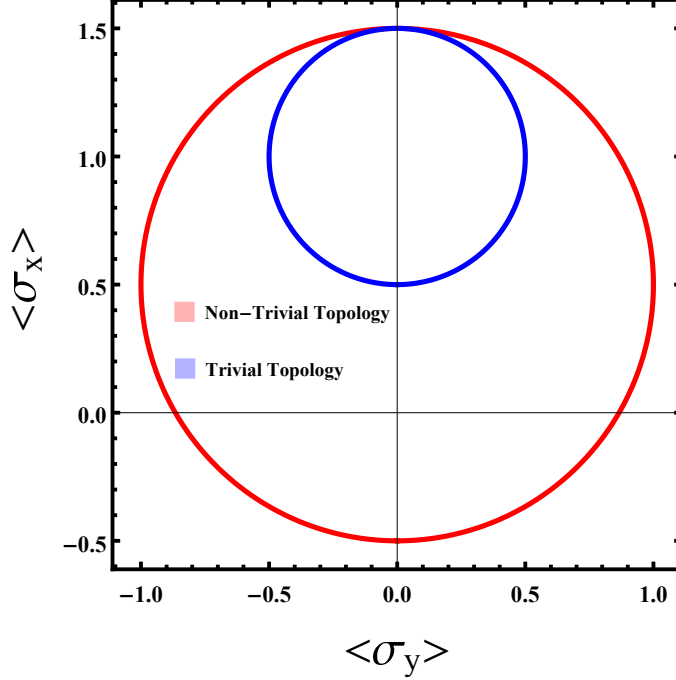


Figure 1.5: Topological characterization of the Hermitian system. plot shows the trace of the $H(k)$ in xy plane. Where the red circle represent the non-trivial band structure with $c = 1$ and $k = 0.5$, the blue circle represent the trivial band where $c = 0.5$ and $k = 1$.

The topological transport of wave function in the structures is expanded to the non-Hermitian systems where the optical set up can be implemented[24, 25]. In order to generate the robust localized state in different structure there exists a very common scenario in one dimension as follow: that two topologically distinct configuration chain of dimers placed next to each other then at the interface localized mid-gap state emerges[21, 22]. In this case, transition between the topological invariant, Winding number, plays an important role and caused the creation of the robust localized state at the interface since when dimerization occur there would be the gap in the energy band and since both configurations have exactly same band with different topology there is no other way that the modes be connected to each other except the gap closes and reopen again, mid-gap state plays its role and causes two band structures have connection with each other. This is the most general case investigated to generate and explore the properties of the topological structure. Now the question is that, is there any possibility to have

such protected state in the structure while we keep the system in the same topology? In other words, is it necessary that topological invariant of the structure changes for the emergence of the localized state?. While topological properties of the band structure is addressed in the Hermitian systems very well and classification is completely understood, where Hermiticity ensures the existence of the real band structure [26], it still has not been fully understood in the open system. Therefore, investigation on the topological characterization of an open system like PT -symmetric optical structures[27] and topologically protected wave transport with zero energy, attracted lots of interest. This question will be completely addressed in the third part of this thesis.

CHAPTER II

QUANTUM EVOLUTION VIA DIABATIC PROCESS

Currently, because of technological demands and advancement which require, new proposals, and approaches, quantum mechanics is considered as the fruitful framework both in science and engineering. Since, it provides a flexible platform to control and manipulate the systems for developing and applying engineering, which makes quantum science an important matter with widespread applications[28, 29, 30, 31, 32, 33, 34]. Generally, we can find many diverse things that depend on quantum physics for their operation. For instance, computer industry, quantum information processing, and quantum control, where all need system or state preparation . The quantum adiabatic theorem is considered as the most promising way to manipulate and modify the parameters of a system to reach out the desired setup. Moreover, there would be no doubt in the correctness of adiabatic theorem as well. However, to apply changes on the system, fast passages are more desirable. In addition, satisfying the necessary condition of the adiabatic theorem is hard to realize from a practical standpoint. Here in this chapter, we will address the demand to find a fast approach for system manipulation, while we look for the same result as the counter adiabatic process. The structure of the present chapter is as follows: First, we review the adiabatic process and the theorem which is the promising passage to prepare the finalized desired state. However, the process takes a long time and the conditions are hard to satisfy. Then, we explore the alternative approaches to speeding up the adiabatic passage called " shortcut to adiabaticity", through which the preparation time is reduced. Meanwhile, we clarify the physics of population transfer. Although the shortcut technique sacrifices the thermodynamic cost for speeding up the process, it provides the fast passage to prepare the desired quantum state. Finally, we introduce a new approach that not

only removes the constraint of shortcut to adiabaticity dynamically, but also we claim the cited approach should be considered as the time-optimal process available for quantum state preparation.

2.1 General overview on Adiabatic Evolution

In quantum mechanics, the time evolution of the wave function is determined by the self-adjoint operator called Hamiltonian. Therefore, one needs to look into the Hamiltonian to explore how the system evolves by solving the time-dependent Schrödinger equation

$$i\hbar\partial_t\psi(t) = H(t)\psi(t) \quad (2.1)$$

where $\hbar = 1$ and $\psi(t)$ is the eigenstate of the system and a vector in Hilbert space.

In the case of the gradual applied changes, the system follows the adiabatic process which gives an approximate solution to the Schrödinger equation and tracks its dynamical effect. Adiabatic theorem first mentioned by Ehrenfest[35], then Born and Fock presented the first proof on it [36].As mentioned in the introduction, according to adiabatic assumption, the time dependency of any state expanded by the instantaneous eigenstate expressed with

$$|\psi(t)\rangle = \sum e^{i\theta_n(t)} e^{i\gamma_n(t)} |n(R(t))\rangle \quad (2.2)$$

substitution Equation.2.2 in Equation.2.1 leads to

$$\begin{aligned} \frac{d}{dt}\gamma_n(t)e^{i\gamma_n(t)}e^{i\theta_n(t)} &= \sum ie^{i\theta_n(t)}e^{i\gamma_n(t)}\langle n(R(t))|\frac{\partial}{\partial t}|m(R(t))\rangle \\ &= ie^{i\theta_n(t)}e^{i\gamma_n(t)}\langle n(R(t))|\frac{\partial}{\partial t}|n(R(t))\rangle + \sum ie^{i\theta_n(t)}e^{i\gamma_n(t)}\langle n(R(t))|\frac{\partial}{\partial t}|m(R(t))\rangle \end{aligned} \quad (2.3)$$

If we ignore transition to the other eigenstates which is the desired result of adiabatic theorem, we reach the equation of the Berry phase Equation.1.4. In addition to the emergence of the Berry phase, in fact adiabatic theorem plays an important role in other fields of physics ranging

from molecular physics [28, 29, 30, 31, 32, 33, 34], quantum Hall physics [34, 37], quantum annealing [38, 39, 40] and quantum simulation [41]. However, slow successive modification in parameters, makes the adiabatic process as one of the time-consuming procedures. So, here one natural question arises: Would it be possible to make the process faster while the output does not change?

2.2 Alternative Approaches to Adiabatic Population Transfer

Complete population transfer is one of the contexts that adiabatic theorem is applicable when inversion occurs from one specific state of the time-dependent Hamiltonian to the other eigenstate of Hamiltonian at $t \rightarrow \infty$. The term "population transfer", specifically refers to, transferring the atom or molecule in a specified discrete quantum state, to another quantum state. However, during the long time evolution, there is always a high probability that the system exposed to the noise and non-adiabatic couplings which spoil the efficiency of population transfer. Therefore, in order to improve the population inversion from the ground state (GS) of a system to the GS of a new system, some techniques have been proposed, including nonlinear level-crossing [42], amplitude-modulated and composite pulses [43, 44], optical and laser-induced adiabatic rapid passage [45, 46] and parallel adiabatic passage [47]. In addition to these techniques, the growing method called shortcut to adiabaticity (STA) has been used. In the context of STA, speeding up the process is desired, while the goal is to keep the evolution of a wave function under a controlled process. STA constitutes a protocol through the non-adiabatic pattern, use the counter diabatic driving field [48, 49, 50, 51], while it provides the same population transfer and the final state as the adiabatic counterpart does. Therefore, its application spans a broad range from ultracold atoms [52, 53], Superconducting qubits [54] and quantum thermodynamics [55, 56, 57, 58, 59], to optical physics, such as fast transport of populations [60], in the classical realm. However, most of the alternative approaches are suggested in the Hermitian system while the non-Hermitian Hamiltonian provides a faster process [61].

A very good example to realize population transfer is a particle in the quadratic potential,

$U = \frac{1}{2}m\omega^2x^2$. Suppose we change the frequency to the final value $\frac{\omega^2}{2}$. Based on how fast we change the functional form of the potential, either population transition may happen or not. Then, in the latter case, we end up with a superposition state Figure(2.1). In the left figure, the system is prepared in the GS of a Hamiltonian, while in the right figure, as the applied change does not follow the adiabatic condition, the system has is a superposition final state. That is the situation occurs when the process follows the diabatic condition. Meanwhile, the goal of STA is to force the undesired configuration change into the one with the whole probability amplitude in GS.

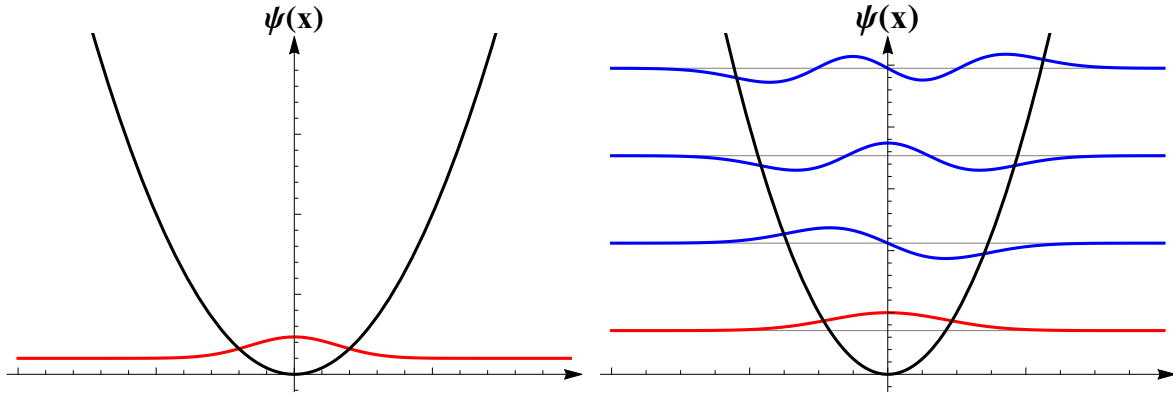


Figure 2.1: Left figure shows the ground state of a particle in quadratic potential $U = \frac{1}{2}m\omega^2x^2$. While, the right figure represent the first four stationary state of the particle in the $U = \frac{1}{2}m\frac{\omega^2}{2}x^2$ when the potential changes so rapidly, caused the final state be a superposition state.

2.3 Landau-Zener Formalism, The Spirit Of The Population Transfer

A very good example illustrates the physics of population transfer completely is a simple model called Landau-Zener (LZ), briefly reviewed in this section,. LZ covers the probability of (non-)adiabatic population transfer [62, 63]. In particular case, consider a two-level Hermitian system controlled by the Equation.2.1. Generally, for the two-level system, the $\psi(t)$ could be written as the superposition of two basis as, $|\psi(t)\rangle = c_1(t)|0\rangle + c_2(t)|1\rangle$ where, $|c_{1,2}(t)|^2$ determines the probability of finding a particle in each state. Moreover, $|0\rangle = (0, 1)^T$ and $|1\rangle = (1, 0)^T$ are basis of the Hilbert space, where T denotes the transposition. Now lets

consider the dynamics of a two-level coupled LZ system as

$$\begin{aligned}
 i\partial_t \psi_1(t) &= -\varepsilon^2 t \psi_1(t) + k \psi_2(t) \\
 i\partial_t \psi_2(t) &= \varepsilon^2 t \psi_2(t) + k \psi_1(t)
 \end{aligned} \tag{2.4}$$

Therefore, the Hamiltonian expressed by the following Hermitian matrix as

$$H = \frac{\hbar}{2} \begin{pmatrix} -\varepsilon^2 t & k \\ k^* & \varepsilon^2 t \end{pmatrix} \tag{2.5}$$

where ε defines how fast or slow the Hamiltonian changes through the time and interaction strength of two levels or coupling denoted by k . First, consider we set the coupling to be zero.

The Hamiltonian forms a diagonal matrix as

$$H = \frac{\hbar}{2} \begin{pmatrix} -\varepsilon^2 t & 0 \\ 0 & \varepsilon^2 t \end{pmatrix} \tag{2.6}$$

where the elements of the matrix are the eigenvalues of the Hamiltonian satisfy the eigenvalue-eigenvector equation with exact solutions as following

$$\begin{aligned}
 |\psi_1(t)\rangle &= \exp\left(\frac{1}{\hbar} \int_0^t E_1(t') dt'\right) |0\rangle \\
 |\psi_2(t)\rangle &= \exp\left(\frac{1}{\hbar} \int_0^t E_2(t') dt'\right) |1\rangle
 \end{aligned} \tag{2.7}$$

It is clear from the Hamiltonian in Equation .2.6 that the vectors $|0\rangle$ and $|1\rangle$ are the eigenvectors of the Hamiltonian through all times. Besides, the energy level of the system cross and that is not the case generally happens. The Hamiltonian should have a special form, left Figure (2.2). Now, lets look at a little bit more complicated situation when the states are coupled to each other through a constant off diagonal term as k in Equation.2.5. We choose the

coupling be equal to 1. Then, the eigenvalues of 2.5 are

$$E_{\pm}(t) = \pm\sqrt{1 + (\varepsilon^2 t)^2} \quad (2.8)$$

If we look at $t = 0$, the eigenvalues are $E = \pm|k|$. Interestingly, at $t \rightarrow \infty$ the diagonal terms are dominant. However, the coupling parameter in the coupled states avoid crossing of the eigenstates for small value of time. Then the energy diagram of the system looks alike the right Figure (2.2)

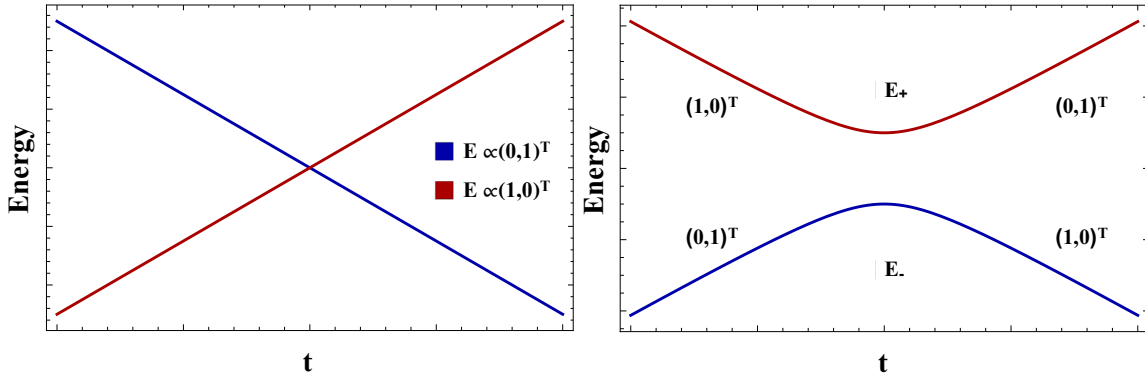


Figure 2.2: Left figure: Bare energy corresponding to the states $|0\rangle$ and $|1\rangle$ crossing through the time in Landau- Zener Model. Right figure: Bare energy corresponding to the states $|0\rangle$ and $|1\rangle$ in the Landau- Zener Model adiabatic transition, while the coupling between the states avoids crossing.

The parameter ε in Equation.2.5 controls the dynamics of the system whether it follows the adiabatic passage or diabatic one. However, the probability amplitudes in the adiabatic basis $|\psi_{adiabatic}\rangle$ and dibatic basis $|\psi_{diabatic}\rangle$ could be connected via rotation,

$$\psi_{diabatic}(t) = R(\theta)\psi_{adiabatic}(t) \quad (2.9)$$

Substitution of the Equation.2.9 in Equation.2.1 leads to

$$i\psi_{diabatic}(t) = (R^{-1}(\theta)HR(\theta) - iR^{-1}(\theta)\dot{R}(\theta))\psi_{adiabatic}(t) \quad (2.10)$$

Where the rotation matrix $R(\theta)$ is defined as

$$R(\theta) = \begin{pmatrix} \cos(\theta) & \sin(\theta) \\ -\sin(\theta) & \cos(\theta) \end{pmatrix} \quad (2.11)$$

While we consider $\theta = \frac{1}{2} \arctan\left(\frac{1}{\varepsilon^2 t}\right)$ and define the

$H_{adiabatic}(t) = (R^{-1}(\theta)HR(\theta) - iR^{-1}(\theta)\dot{R}(\theta))$, written in matrix form as following

$$H(t) = \begin{pmatrix} E_-(t) & -i\dot{\theta}(t) \\ i\dot{\theta}(t) & E_+(t) \end{pmatrix} \quad (2.12)$$

If the $|\dot{\theta}(t) = \frac{1}{2} \left(\frac{-\varepsilon^2}{(\varepsilon^2 t)^2 + 1} \right)| \ll \Delta E_{\pm}$, the evolution is adiabatic. then

$$|\Psi_{adiabatic}(-\infty)\rangle = |0\rangle, \quad |\Psi_{adiabatic}(\infty)\rangle = |1\rangle \quad (2.13)$$

Suppose at the initial time $t = t_i = -\infty$, the system is prepared in GS $|0\rangle$ so : $c_1(t_i) = 1$ and $c_2(t_i) = 0$. As the Hamiltonian is time-dependent, after evolution at the other extreme point $t = t_f = \infty$, the GS flips to the $|1\rangle$. As mentioned earlier, ε defines the speed of changes in the Hamiltonian. When the ε is small, the system undergoes changes through the adiabatic passage. Therefore, the population in the initial state $|0\rangle$ is completely transferred over to the $|1\rangle$ for the gradual changes. For the large value of ε , evolution follows the non-adiabatic passage so, there would not be enough time for level crossing and population transfer does not occur Figure(2.3). As a result of the diabatic process and the existence of non-adiabatic channels, the efficiency of complete population transition reduces. While different methods have been presented in the section (2.2) focused on improvement in the efficiency of two states connection, in the next section we will briefly review one example.

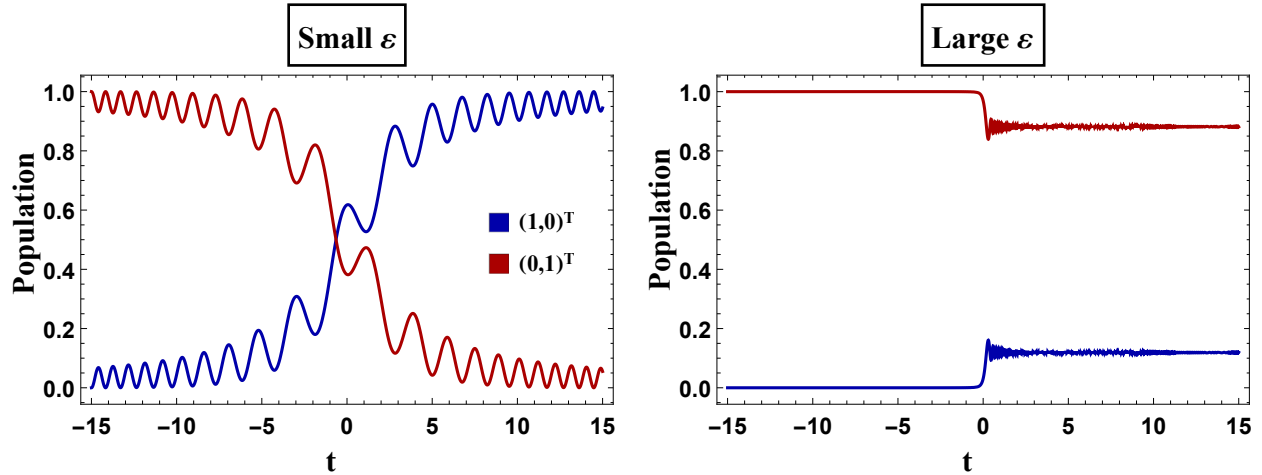


Figure 2.3: Time evolution of population transfer in the Landau-Zener Model for the two-level system. (left figure) shows the ground states flips from state $|0\rangle$ to $|1\rangle$ under the adiabatic passage. Right figure represents non-level crossing evolution of states under the non-adiabatic passage.

2.4 Non-Hermitian Shortcut to Adiabaticity

So far, to address the population inversion most of the approaches focused on the Hermitian and closed system. Specifically, in the previous section, we reviewed the coupled two-level system where the complete population transfer under the adiabatic passage observed.

Moreover, in the non-adiabatic passage with the cost of increasing the coupling between the states, transporting of the probability amplitude is possible Figure(2.4).

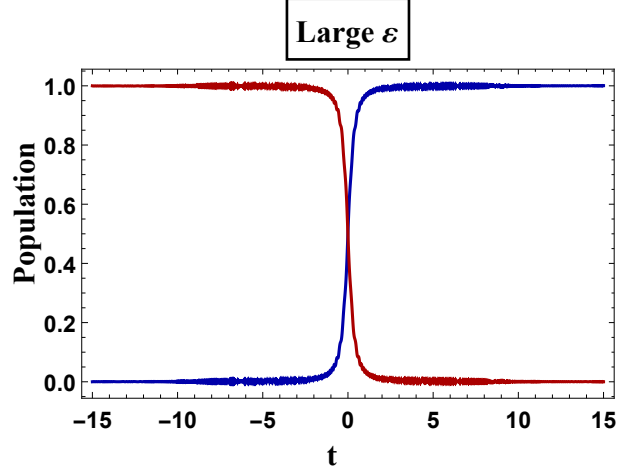


Figure 2.4: Time evolution of population transfer in the Landau-Zener model for the two-level system, while we speed up the process $\varepsilon = 5$ and increase the coupling or interaction strength of the two state to $k = 10$.

Recently, a growing approach called Shortcut To Adiabaticity (STA) attracted lots of interest due to the broad application, like quantum information processing and quantum control. In this section, we will review one of the examples. The main goal in STA is to cancel out the non-adiabatic coupling contribution during the transit time to the target state [64]. Therefore, to realize the population inversion, in the following example, an extra non-Hermiticity part has been added as $i\gamma(t)$ term to the Hermitian Hamiltonian like Equation.2.5. The implementation of non-Hermiticity as the external field makes the population inversion possible. As a result, we obtain

$$H^\gamma(t) = \frac{\hbar}{2} \begin{pmatrix} -\varepsilon^2 t + i\gamma(t) & 1 \\ 1 & \varepsilon^2 t - i\gamma(t) \end{pmatrix} \quad (2.14)$$

and the Hamiltonian in the adiabatic basis takes the form[65]

$$H_a^\gamma(t) = \hbar \begin{pmatrix} E_-(t) + \frac{1}{2}i\gamma(t)\cos(2\theta) & \frac{1}{2}i\gamma(t)\sin(2\theta) - i\dot{\theta}(t) \\ \frac{1}{2}i\gamma(t)\sin(2\theta) + i\dot{\theta}(t) & E_+(t) - \frac{1}{2}i\gamma(t)\cos(2\theta) \end{pmatrix} \quad (2.15)$$

where the $E_{\pm}(t)$ is defined in Equation.2.8. As it is clear in the Hamiltonian in Equation.2.15, there exist diabatic coupling terms prevent complete population transfer to the desired state. The non-adiabatic coupling has the Lorentzian functional form as

$$\dot{\theta}(t) = -\frac{2\varepsilon^2 t}{2(\varepsilon^2 t)^2 + 1} \quad (2.16)$$

Hence, we choose the non-Hermitian external field with the following form

$$\gamma(t) = \frac{2\dot{\theta}(t)}{\sin(2\theta)(t)} = -\frac{\varepsilon}{2\sqrt{\frac{1}{\varepsilon^2} + (\varepsilon^2 t^2)}} \quad (2.17)$$

to nullify the population leakage into other states and force to have the whole population in the target state. The STA in non-Hermitian system used more often since it provides fast passage even when the coupling between the states is small[64]. The implementation of the shortcut to adiabaticity (STA) and investigating the external driving field can be accomplished in the system of two coupled optical waveguides with gain/loss profile and propagation constant that varies with distance(time)[66].

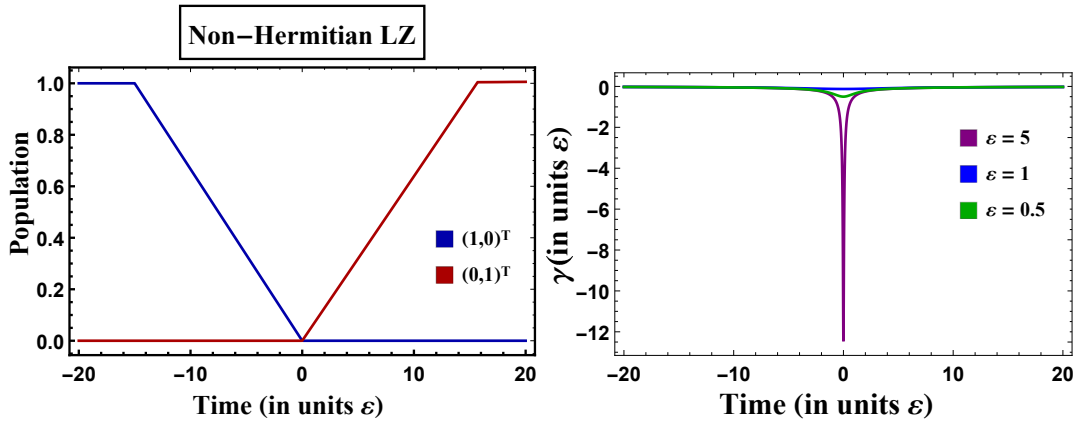


Figure 2.5: Evolution of population and transition between the ground state in the non-Hermitian LZ model (left plot). external field or γ function with respect to time and for different values for parameter ε which defines the speed of the diabatic process.[65]

To sum up, shortcut techniques both in the Hermitian case and non-Hermitian system come with the problem of either increasing the coupling or adding more gain into the system to cancel the effect of speeding up the process. In addition, in the case of non-Hermitian the functional form of the gain profile might not be simple to generate in lab. So, it means spending more energy and consequently more money to reach the same result of the adiabatic passage through non-adiabatic one.

2.5 Dynamical Approach to Low-Cost Shortcut to Adiabaticity(DASA)

In the previous section, we review one example of the STA approach, designed to speed up the quantum adiabatic process. However, the STA protocol encounters difficulties. Firstly, due to the high thermodynamic cost of the process. Secondly, the challenge of the extra field creation. So up to here, the problem is to make the population inversion between GS faster while the Hamiltonian at $T = 0$ undergoes changes till the final form at $T = t$. In a real system most of the time during time evolution, because of environment interaction and existence of the non-adiabatic channel, we face the open system and can not meet the necessary conditions of the adiabatic process. However, it is important not only to bypass the thermodynamic cost of the shortcuts aiming to cancel out the undesired channel but also to find the scenario with a more experimental friendly platform that addresses the population transfer between ground states. As we try not to perturb the other states, we focus on the dynamical properties of the system in such a way that every previous obstacle removes differently. Therefore, let us consider a time-independent two-level non-Hermitian Hamiltonian with the following form

$$H = \begin{pmatrix} \omega_1 + i\gamma_1 & 1 \\ 1 & \omega_2 + i\gamma_2 \end{pmatrix}. \quad (2.18)$$

in the above Hamiltonian, the $\omega_{1,2}$ and $\gamma_{1,2}$ are real parameters. We normalized the on-site potential $\omega_{1,2} + i\gamma_{1,2}$ to the coupling between the states. The Hamiltonian in Equation(2.18) generally has been used to model, for example, light propagation in the coupled waveguides

and resonators with gain and loss [67, 68] and dynamics of open systems[69, 70]. The time-evolution operator for such a time-independent system is given by e^{-iHt} . If we apply the evolution operator on the initial state. a supper position state, $|\psi(0)\rangle$, in the Hamiltonian's basis, evolves according to

$$|\psi(t)\rangle = e^{-iHt}|\psi(0)\rangle = c_1e^{-i\lambda_1t}|\lambda_1\rangle + c_2e^{-i\lambda_2t}|\lambda_2\rangle. \quad (2.19)$$

where $\lambda_{1,2}$ and $|\lambda_{1,2}\rangle$ are the eigenvalues and corresponding eigenvectors of the Hamiltonian. In order to observe population inversion, the initial state with whole amplitude needs to experience decay and the other one should encounter amplification, so according to Equation(2.19) the eigenvalues play an important role in the evolution of the state. Therefore, our goal is to focus on setting and engineering the eigenvalues such that one of them caused decay/amplification in one of the eigenvectors while the other keeps the amplitude on its corresponding eigenstate unchanged. Based on the form of contribution of $\lambda_{1,2}$ in Equation(2.19) if we impose the following constraint decay/amplification is realized

$$\lambda_1 = x_1 + iy, \quad \lambda_2 = x_2 \quad (2.20)$$

where $x_{1,2}$ and y are some real parameters that we aim to find them. We introduce the diagonalized matrix H_d which has only eigenvalues of the matrix H in the main diagonal and then look for matrix R such that

$$H = R^{-1}H_dR, \quad R \equiv \begin{pmatrix} a & b \\ c & d \end{pmatrix} \quad (2.21)$$

specifically R is the matrix constructed of the two eigenvectors of H and R^{-1} is the inverse matrix of R . From the similarity transformation in Equation(2.21), $a = -\frac{bd}{c}$. Then by replacing a in Equation(2.21) and solving for parameter d , we get two solutions of the following form

$d = \pm \frac{c\sqrt{-i\gamma_1+x_2-\omega_1}}{\sqrt{i\gamma_1-x_1-iy+\omega_1}}$ or $d = \pm \frac{c\sqrt{x_1+i(-\gamma_2+y+i\omega_2)}}{\sqrt{i\gamma_2-x_2+\omega_2}}$. Since d should be unique, we put these solutions equal and solve the equation for another parameter, γ_1 , and get $\gamma_1 = -\gamma_2 + i(\omega_1 + \omega_2 - x_1 - x_2) + y$. However, γ_1 should be real, thus, $(\omega_1 + \omega_2 - x_1 - x_2) = 0$. Accordingly,

$$x_1 + x_2 = \omega_1 + \omega_2, \quad y = \gamma_1 + \gamma_2. \quad (2.22)$$

By using Equation(2.22) in addition to the fact that the coupling, off-diagonal term, in Equation(2.21) should be real we reach to the solutions for $x_{1,2}$ as follow

$$x_1 = \frac{\omega_1\gamma_1 + \omega_2\gamma_2}{\gamma_1 + \gamma_2}, \quad x_2 = \frac{\omega_1\gamma_2 + \omega_2\gamma_1}{\gamma_1 + \gamma_2}. \quad (2.23)$$

So far, we find the parameters a , d , y and $x_{1,2}$, by plugging in the solutions of the Equation(2.23) into Equation(2.21), we can look for the solutions for the other remaining parameter b which head to two results as

$$b = \frac{-iay}{\gamma_1(y - i\Delta\omega)}$$

$$b = \frac{a\gamma_2(iy - \Delta\omega)}{y} \quad (2.24)$$

where $\Delta\omega = \omega_1 - \omega_2$. again, as b is a unique parameter when we set the two solutions in Equation(2.24) equal. Then, we get three different solutions for parameter γ_1 namely, $g_{1,2,3}$ as a function of $\Delta\omega$ and γ_2 .

$$\begin{aligned}
\gamma_1 = g_1(\Delta\omega, \gamma_2) &= \frac{1}{6\gamma_2} (-2 - 4\gamma_2^2 - (2i\sqrt[3]{2}(\gamma_2^2(\gamma_2^2 - 3\Delta\omega^2) - 2\gamma_2^2 + 1)) / (-6i\gamma_2^4(1 - 3\Delta\omega^2) \\
&+ 3i\gamma_2^2(3\Delta\omega^2 + 2) + 3\sqrt{3} \\
&\sqrt{\gamma_2^4\Delta\omega^2(-4\gamma_2^2(\gamma_2^2 + \Delta\omega^2))^2 + 4\gamma_2^2(3\gamma_2^2 - 5\Delta\omega^2) - 12\gamma_2^2 + \Delta\omega^2 + 4}) \\
&+ 2i\gamma_2^6 - 2i)^{1/3}) \\
&+ i2^{2/3}(-i(-2\gamma_2^4(\gamma_2^2 + 9\Delta\omega^2) + 3\gamma_2^2(2\gamma_2^2 - 3\Delta\omega^2) - 6\gamma_2^2 + 2) \\
&+ 3\sqrt{3}\sqrt{\gamma_2^4\Delta\omega^2(-4\gamma_2^2(\gamma_2^2 + \Delta\omega^2))^2 + 4\gamma_2^2(3\gamma_2^2 - 5\Delta\omega^2) - 12\gamma_2^2 + \Delta\omega^2 + 4}) \\
&^{1/3}), \\
\gamma_1 = g_2(\Delta\omega, \gamma_2) &= -\frac{1}{12\gamma_2} (4(2\gamma_2^2 + 1) + 2\sqrt[3]{2}(\sqrt{3} - i)(\gamma_2^2(\gamma_2^2 - 3\Delta\omega^2) - 2\gamma_2^2 + 1) / \\
&(-6i\gamma_2^4(1 - 3\Delta\omega^2) + 3i\gamma_2^2(3\Delta\omega^2 + 2) + 3\sqrt{3}(\gamma_2^4\Delta\omega^2(-4\gamma_2^2(\gamma_2^2 + \Delta\omega^2))^2 \\
&+ 4\gamma_2^2(3\gamma_2^2 - 5\Delta\omega^2) - 12\gamma_2^2 \\
&+ \Delta\omega^2 + 4))^{1/2} + 2i\gamma_2^6 - 2i)^{1/3} + 2^{2/3}(\sqrt{3} + i) \\
&(-i(-2\gamma_2^4(\gamma_2^2 + 9\Delta\omega^2) + 3\gamma_2^2(2\gamma_2^2 - 3\Delta\omega^2) - 6\gamma_2^2 + 2) \\
&+ 3\sqrt{3}\sqrt{\gamma_2^4\Delta\omega^2(-4\gamma_2^2(\gamma_2^2 + \Delta\omega^2))^2 + 4\gamma_2^2(3\gamma_2^2 - 5\Delta\omega^2) - 12\gamma_2^2 + \Delta\omega^2 + 4}) \\
&^{1/3}), \\
\gamma_1 = g_3(\Delta\omega, \gamma_2) &= \frac{1}{12\gamma_2} (-4(2\gamma_2^2 + 1) + 2\sqrt[3]{2}(\sqrt{3} + i)(\gamma_2^2(\gamma_2^2 - 3\Delta\omega^2) - 2\gamma_2^2 + 1) / \\
&(-6i\gamma_2^4(1 - 3\Delta\omega^2) + 3i\gamma_2^2(3\Delta\omega^2 + 2) - 2i + 2i\gamma_2^6 + 3\sqrt{3} \\
&(\gamma_2^4\Delta\omega^2(-4\gamma_2^2(\gamma_2^2 + \Delta\omega^2))^2 - 12\gamma_2^2 + \Delta\omega^2 + 4 + 4\gamma_2^2(3\gamma_2^2 - 5\Delta\omega^2)))^{1/2})^{1/3} \\
&+ 2^{2/3}(\sqrt{3} - i)(-i(-2\gamma_2^4(\gamma_2^2 + 9\Delta\omega^2) + 3\gamma_2^2(2\gamma_2^2 - 3\Delta\omega^2) - 6\gamma_2^2 + 2) + 3\sqrt{3} \\
&(\gamma_2^4\Delta\omega^2(-4\gamma_2^2(\gamma_2^2 + \Delta\omega^2))^2 + 4\gamma_2^2(3\gamma_2^2 - 5\Delta\omega^2) - 12\gamma_2^2 + \Delta\omega^2 + 4))^{1/2})^{1/3}) \\
&\hspace{15em} (2.25)
\end{aligned}$$

These solutions give us information about the amount of gain and loss we are allowed to put into the Hamiltonian in order to have the special form of the eigenvalues namely, one being

totally real and the other being complex. The functional form of all three $g_{1,2,3}$ depends on $\Delta\omega$ in their denominator, thus there would not exist, such Hamiltonian when $\Delta\omega = 0$. Moreover, $g_{1,2,3}$ depend on the square power of the $\Delta\omega$, therefore, γ_1 is invariant under the change of the sign in the $\Delta\omega$. Finally, unlike the complicated functional form of the $g_{1,2,3}$, they are time-independent and which makes them be just some constants in transit time. In Figure(2.6), the real and imaginary part of the solution for γ_1 has been plotted with respect to the γ_2 . The plot shows an accepted domain of each function. We should be careful when we select the value for our physical parameter, γ_1 , as γ_1 should be real. So, there is no restriction on choosing a value from g_1 since it is a real function. However, the other two functions are complex.

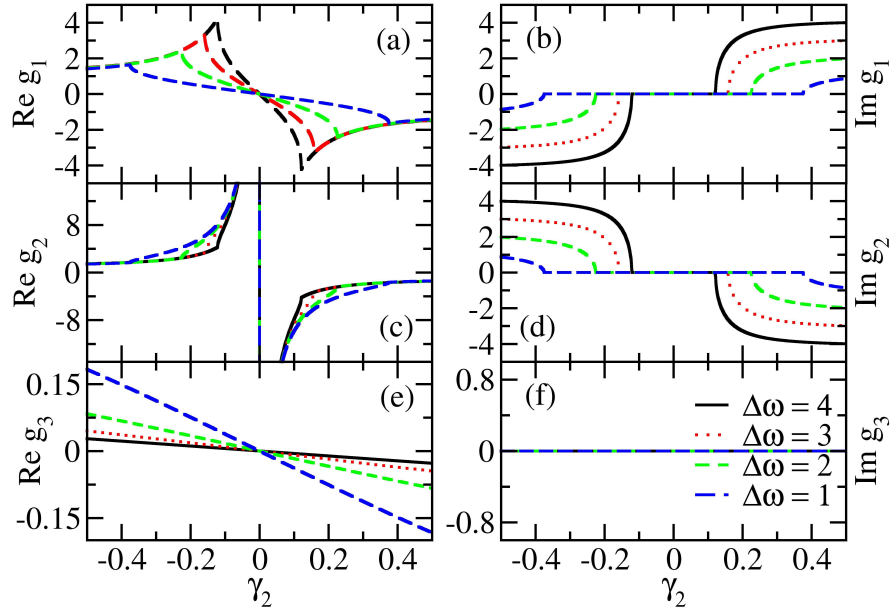


Figure 2.6: Real (left column) and imaginary (right column) part of the $g_{1,2,3}$ as a function of the γ_2 for $\Delta\omega = 1, 2, 3, 4$. All region make the g as the real function are acceptable. fore instance, we do not have restriction on choosing the correct value fom g_3 , as it is a real function. As the other functions are generally complex, the accepted values are the one make the imaginary part equal to zero. Therefore, one eigenvalues of Hamiltonian in Equation.(2.18) becomes absolutely real and the other one becomes complex. Figure is taken from [71]

Now we have all the necessary parameters to calculate the eigenvalues and corresponding

eigenvectors which have the following forms

$$\lambda_1 = \frac{\omega_1 \gamma_1 + \omega_2 \gamma_2}{\gamma_1 + \gamma_2} + i(\gamma_1 + \gamma_2), \quad \lambda_2 = \frac{\omega_1 \gamma_2 + \omega_2 \gamma_1}{\gamma_1 + \gamma_2} \quad (2.26)$$

$$|\lambda_1\rangle = \begin{pmatrix} \frac{y}{\gamma_2(iy - \Delta\omega)} \\ 1 \end{pmatrix}, \quad |\lambda_2\rangle = \begin{pmatrix} 1 \\ \frac{-\gamma_1(\Delta\omega + iy)}{y} \end{pmatrix}. \quad (2.27)$$

Then, it is important to look at the population transfer between the lower and higher energy state. According to the Equation(2.19) and (2.26), the imaginary sign of λ_1 becomes important and determines the dynamics of the corresponding state. When the $\gamma_1 + \gamma_2 < 0 (> 0)$ the state experiences decay (amplification). Meanwhile, the amplitude in other state with real eigenvalue λ_2 , remains constant and the coefficient is just adding a phase to the state. The rest of the present section allocated to explain, how population from GS of initial Hamiltonian transfer to GS of the final Hamiltonian with our proposed non-Hermitian Hamiltonian.

First, we need the ground state to be $|1\rangle \approx (0, 1)^T$ at the initial time. Besides, the dissipation should occur in the ground state. Therefore, we need to set the parameters of the Hamiltonian in Equation(2.18) such that the values of the $\Sigma\gamma$ be negative while the other eigenvector posses the real eigenvalue which keeps the small initial amplitude in the higher energy state constant. When the amplitude in the $|1\rangle$ nullify, our task is to amplify the initial population in state $|2\rangle$. Meanwhile, the ground state also should flip from $|1\rangle$ to $|2\rangle$. lets look at the Equation(2.26), if $|\gamma_2| > |\gamma_1|$, $\gamma_{2(1)} < (>)0$, and $\omega_2 < 0$ then $|\lambda_1\rangle$ is the lower energy level. One can show that if $|\gamma_1 + \gamma_2| \ll |\omega_2|$ then $|\lambda_1\rangle \approx (0, 1)^T = |1\rangle$. Similarly, using the same equations one can show that for $\omega_2 = 0$, $\omega_1 \approx 0$, and $\gamma_1 > |\gamma_2| \approx 0$, where both $\omega_1, \gamma_2 < 0$, the eigenstate $|\lambda_1\rangle \approx |2\rangle = (1, 0)^T$ becomes the lower energy level and undergoes an exponential amplification. The dynamical evolution of the system under such condition, for the Hamiltonian in Equation.2.1 is represented by the following coupled differential equation as

$$\begin{aligned}
i\partial_t \psi_1(t) &= (\omega_1 + i\gamma_1)\psi_1(t) + \psi_2(t) \\
i\partial_t \psi_2(t) &= (\omega_2 + i\gamma_2)\psi_2(t) + \psi_1(t)
\end{aligned} \tag{2.28}$$

where the excited state at the initial time $t = -15$ be $|1\rangle$ and the associated Hamiltonian through the evolution time considered as $\mathcal{H}_{2 \times 2}(t) = H_1 \times (\Theta(t + 15) - \Theta(t + 12)) + H_2 \times (\Theta(t + 12) - \Theta(t + 11.358)) + \mathbf{1} \times \Theta(t + 11.358)$ in which $\Theta(x) = \begin{cases} \mathbf{0} & \text{if } x < 0 \\ \mathbf{1} & \text{if } x > 0 \end{cases}$ is the Heaviside step function matrix and the parameters in $H_{1,2}$ numerically chosen to be $\omega_1 + i\gamma_1 = 0 + ig_3(10, -0.95)$, $\omega_2 + i\gamma_2 = -10 - 0.95i$. We chose the parameters in H_1 and in H_2 as the following: $\omega_1 + i\gamma_1 = -0.01 + ig_2(-0.01, -0.25)$, $\omega_2 + i\gamma_2 = 0 - 0.25i$.

To sum up this section, as it is illustrated in the Figure (2.7), in two steps $\mathcal{H}_{2 \times 2}(t)$ transition and population inversion from the initial GS to the target GS is observed. The basis of our general Hamiltonian in Equation(2.18) are almost parallel to the $|1\rangle$ and $|2\rangle$. We start with the configuration that majority of the population are placed into the initial ground state and a little kept in the other eigenstate then, it is just important how we choose our set of parameters. The imaginary part of the complex eigenvalue makes difference in dynamics, namely, caused the decay or amplification in the expected eigenvector. Finally, our desired target state as the GS with whole population by means of a fast diabatic protoc is achieved.

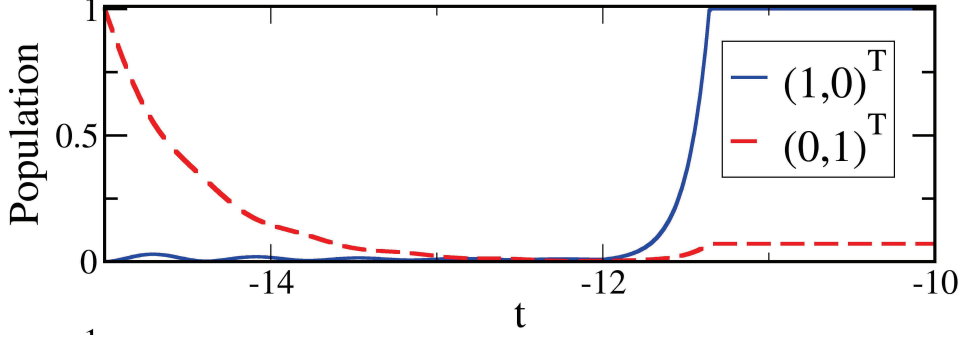


Figure 2.7: Amplitude probability of the bare states $(0,1)^T$ and $(1,0)^T$ as a function of time (in the unit of coupling) using the Hamiltonian $\mathcal{H}_{2 \times 2}(t)$. Figure is taken from [71]

2.6 Extension To Higher Dimension

In this section, we extend DASA to the higher dimension and show one can reach the complete population transfer in no time. To address this aim, we begin our analysis by working on the three-level system, extension to other dimensions would be easy. In fact, we Use the Landau-Zener model and write the Hamiltonian for a three-level system in the following form

$$H_{LZ}(\varepsilon, \beta, t) = \begin{pmatrix} -\varepsilon^2 t & \kappa_{12} & \kappa_{13} \\ \kappa_{12}^* & \beta & \kappa_{23} \\ \kappa_{13}^* & \kappa_{23}^* & \varepsilon^2 t \end{pmatrix} \quad (2.29)$$

where κ_{ij} is the coupling between levels i and j and β is the on-site energy level of the middle state. Assume that $\kappa_{12} = \kappa_{23}$ and like the two-level system, we normalize the couplings such that $\kappa_{12} = 1$, and redefine other parameters as $\kappa \equiv \kappa_{13}/\kappa_{12}$, $\mathcal{E}_2 \equiv \beta/\kappa_{12}$, and $t \equiv t/\kappa_{12}$. In the higher dimension the scenario is a little bit different. Since the middle states and its associated parameters, in our example \mathcal{E}_2 and κ , play a crucial role in the adiabatic process of the Landau-Zener model. The effect of these parameters on the dynamics of a three-level system is clearly shown in Figure(2.8 a-d) wherein (a) $\kappa = 0$, $\mathcal{E}_2 = 0$, and $\varepsilon = 0.5$. Although the population transfer to the state $|3\rangle$, there is a significant probability amplitude in the middle state. The contribution of the middle state in the dynamics increases when the value of \mathcal{E}_2 ,

becomes larger. So, the majority of population transfer to the middle state which is not the ground state of the system. Therefore the system does not satisfy the adiabatic condition and we can not reach the final configuration of the adiabatic process while the whole procedure follows slow dynamics Figure(2.8 b). When we decrease the value of ε to $\varepsilon = 0.05$, we ended up with the desired configuration of the adiabatic process Figure(2.8c). However, we sacrifice the speed in order to get the desired transition between the states. On the other hand, when we increase the coupling between $|1\rangle$ and $|3\rangle$, effectively, we suppress the contribution of the middle state in the dynamics of the system. As a matter of fact, the challenging case occurs when the on-site potential of the middle state is large. To understand the mechanism how one can remove the effect of the middle state, let's look at the Schrödinger equation for the 3×3 non-Hermitian system which expressed in the following form

$$i\frac{d}{dt}\Psi = H\Psi, \quad H = \begin{pmatrix} \mathcal{E}_1 & \kappa_{12} & \kappa \\ \kappa_{12}^* & \mathcal{E}_2 & \kappa_{23} \\ \kappa^* & \kappa_{23}^* & \mathcal{E}_3 \end{pmatrix} \quad (2.30)$$

where $\Psi = (\psi_1, \psi_2, \psi_3)^T$, $\mathcal{E}_{1,3} = \omega_{1,3} + i\gamma_{1,3}$ and $\mathcal{E}_2 = \omega_2$. Using the transformation $\psi_j = A_j \exp(-i\mathcal{E}_j t)$ ($i = 1, 2, 3$), we can write the time evolution of the probability amplitudes A_i as

$$i\frac{d}{dt}\mathcal{A} = \begin{pmatrix} 0 & \kappa_{12}e^{i\Delta\mathcal{E}_{12}t} & \kappa e^{i\Delta\mathcal{E}_{13}t} \\ \kappa_{12}^*e^{-i\Delta\mathcal{E}_{12}t} & 0 & \kappa_{23}e^{i\Delta\mathcal{E}_{23}t} \\ \kappa^*e^{-i\Delta\mathcal{E}_{13}t} & \kappa_{23}^*e^{-i\Delta\mathcal{E}_{23}t} & 0 \end{pmatrix} \mathcal{A} \quad (2.31)$$

in which $\mathcal{A} \equiv (A_1, A_2, A_3)^T$ and $\Delta\mathcal{E}_{ij} = \mathcal{E}_i - \mathcal{E}_j$. One can integrate the middle row of Equation.(2.31) and get

$$A_2 = \frac{\kappa_{12}^*}{\Delta\mathcal{E}_{12}} e^{-i\Delta\mathcal{E}_{12}t} A_1 - \frac{\kappa_{23}}{\Delta\mathcal{E}_{23}} e^{i\Delta\mathcal{E}_{23}t} A_3 \quad (2.32)$$

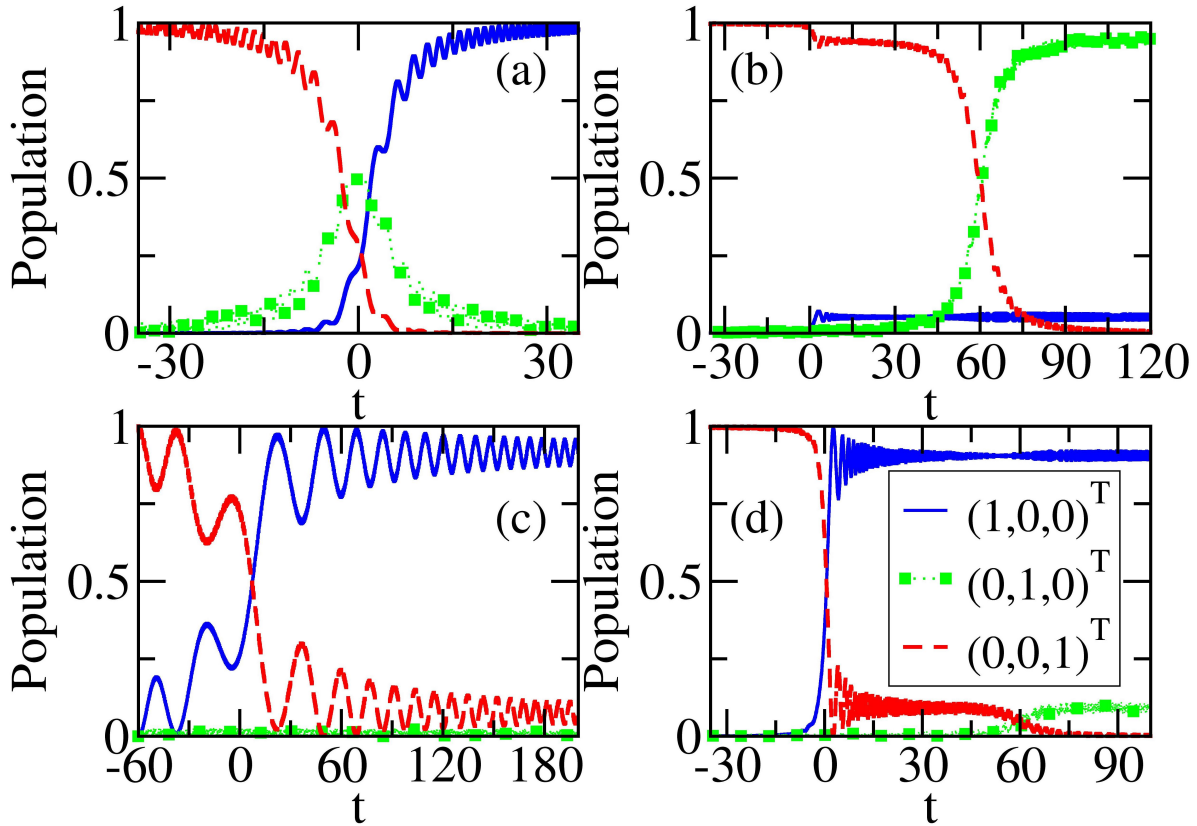


Figure 2.8: Dynamics of a three-level Landau-Zener model (amplitude probability of the bare states $(0,0,1)^T$ and $(0,1,0)^T$, and $(1,0,0)^T$ as a function of time in the unit of outer coupling) associated with the Hamiltonian in Equation.(2.29) for (a) $\kappa = 0$, $\mathcal{E}_2 = 0$, and $\varepsilon = 0.5$, (b) $\kappa = 0$, $\mathcal{E}_2 = 15$, and $\varepsilon = 0.5$, (c) $\kappa = 0$, $\mathcal{E}_2 = 15$, and $\varepsilon = 0.05$, (d) $\kappa = 0.5$, $\mathcal{E}_2 = 15$, and $\varepsilon = 0.5$. We observe that in the absence of strong coupling between the third level and the first level when the on-site potential of the middle level becomes large one needs to make the process much slower in comparison to the two-level system in order to have adiabatic process. Specifically, while for $\varepsilon = 0.5$ one gets a complete population transfer in the two-level system (Figure.2.7 a), as depicted in Figure.(2.8b) for a three-level system with the same ε and $\mathcal{E}_2 = 15$ there wont be any population transfer to the ground state if the first and third level are not directly coupled, namely $\kappa = 0$. Figure is taken from [71]

As the aim was to remove the middle state contribution in the dynamic of the system, population in the A_2 should be zero from Equation.(2.32) when

$$|\Delta\mathcal{E}_{12}| \gg |\kappa_{12}^*|, \quad |\Delta\mathcal{E}_{23}| \gg |\kappa_{23}| \quad (2.33)$$

According to the condition in Equation.(2.33), we make the on-site potential of the middle level large, then the intensity of the middle level is not changing during the dynamics and the system can be effectively described by a two-level system. Specifically, by substituting Equation.(2.32) in Equation.(2.31) we can write a Schrödinger-like equation with a 2×2 effective Hamiltonian that describes the dynamics of the system

$$i \frac{d}{dt} \tilde{\Psi} = H_{eff} \tilde{\Psi}, \quad H_{eff} = \begin{pmatrix} \omega_{12} & k_1 \\ k_2 & \omega_{32} \end{pmatrix} \quad (2.34)$$

where $\tilde{\Psi} = (A_1 e^{-\frac{i\Delta\mathcal{E}_{13}t}{2}}, A_3 e^{\frac{i\Delta\mathcal{E}_{13}t}{2}})^T$, and the elements of the effective Hamiltonian are

$$\omega_{12} = \frac{|\kappa_{12}|^2}{\Delta\mathcal{E}_{12}} + \frac{\Delta\mathcal{E}_{13}}{2}, \quad \omega_{32} = -\frac{|\kappa_{23}|^2}{\Delta\mathcal{E}_{23}} - \frac{\Delta\mathcal{E}_{13}}{2}, \quad k_1 = \kappa - \frac{\kappa_{12}\kappa_{23}}{\Delta\mathcal{E}_{23}}, \quad \text{and} \quad k_2 = \kappa^* + \frac{\kappa_{12}^*\kappa_{23}^*}{\Delta\mathcal{E}_{12}} \quad [72].$$

According to the Equation.(2.34), we are able to reduce the dimension of the system and deal with the effective 2×2 Hamiltonian, if the conditions in Equation.(2.33) is satisfied. Then after, we will be sure about the existence of the system with lower dimension, enable us to use the same dynamical shortcut to reach population transfer in three and higher level system.

Interestingly, not only we have effective 2×2 Hamiltonian produces the same result of the two-level system for population transfer in no time, but also, the same value for the two-level parameters work in three-level population transfer. To check this out, Let us excite the bare state $|1\rangle = (0, 0, 1)^T$ which is the ground state at $t = -15$ and obtain population transfer to the new ground state of the system at $t = 15$, $|3\rangle = (1, 0, 0)^T$ by using the following Hamiltonian

$$\mathcal{H}(t) = H_3 \times (\Theta(t + 15) - \Theta(t + 12)) + H_4 \times (\Theta(t + 12) - \Theta(t + 10.7374)) + \mathbf{1} \times \Theta(t + 10.7374). \quad (2.35)$$

where the two matrices $H_{3,4}$ are constructed based on the parameters used in the corresponding two-level Hamiltonian with the following form

$$H_3 = \begin{pmatrix} 0 + ig_3(10, -0.95) & 1 & 0 \\ 1 & 15 & 1 \\ 0 & 1 & -10 - 0.95i \end{pmatrix} \quad (2.36)$$

and

$$H_4 = \begin{pmatrix} -0.01 + ig_2(-0.01, -0.25) & 1 & 0 \\ 1 & 15 & 1 \\ 0 & 1 & 0 - 0.25i \end{pmatrix} \quad (2.37)$$

If we look at the set of important parameters used to obtain population transfer, for example, $\mathcal{E}_2 = 15$ and $\kappa = 0$. they need a very slow process ($\varepsilon = 0.05$) in order to produce the adiabatic result. While we could easily turn the situation with DASA and get the same outcome as the adiabatic counterpart in much smaller time period

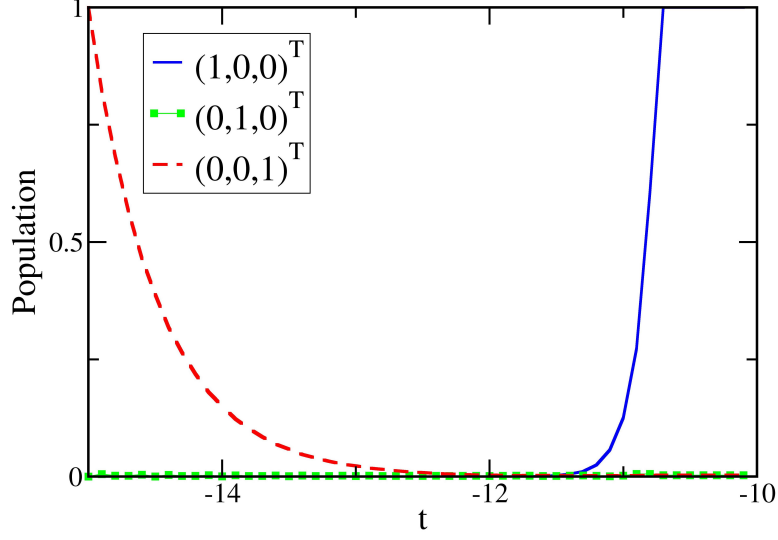


Figure 2.9: Amplitude probability of the bare states $(0,0,1)^T$, $(0,1,0)^T$, and $(1,0,0)^T$ as a function of time using the Hamiltonian in Equation.(2.35) using the same gain and loss parameters that are obtained for the two-level system, namely $\mathcal{H}_{2 \times 2}$ in the main text. We observe that, in a very short time a complete population transfer occurs. Figure is taken from [71]

It is interesting, if we look at the form of the three-level system eigenvalues in each specific Hamiltonian of Equations.(2.36) and (2.37) to see what is going on in the dynamics of the system. Firstly, for H_3 the eigenvalues are

$$\begin{aligned}
 |\lambda_1\rangle \approx |1\rangle &= (0,0,1)^T, & \lambda_1 &\approx -10.04 - 0.948i \\
 |\lambda_2\rangle \approx |2\rangle &= (0,1,0)^T, & \lambda_2 &\approx 15.106 - 0.001i \\
 |\lambda_3\rangle \approx |3\rangle &= (1,0,0)^T, & \lambda_3 &\approx -0.066 + 0.009i
 \end{aligned} \tag{2.38}$$

whereas the eigenvalues for H_4 has the form

$$\begin{aligned}
 |\lambda_1\rangle \approx |3\rangle &= (1,0,0)^T, & \lambda_1 &\approx -0.072 + 3.983i \\
 |\lambda_2\rangle \approx |2\rangle &= (0,1,0)^T, & \lambda_2 &\approx 15.128 + 0.0151i \\
 |\lambda_3\rangle \approx |1\rangle &= (0,0,1)^T, & \lambda_3 &\approx -0.066 - 0.248i
 \end{aligned} \tag{2.39}$$

Although, in three-level system we lose the specific form of the eigenvalues as we have in the two-level system. However, as depicted in Figure(2.9), all complex eigenvalues influence the dynamics of the system such that the result of the dynamics is the same as two-level system. In the first time period $t \in [-15, -12]$ the first eigenvalues which poses larger negative imaginary part, caused decay in the initial ground state almost aligned with $|1\rangle$. The other state parallel to the $|2\rangle$ and $|3\rangle$, experience decay and amplification respectively. $t \in [-12, -10.7374]$, the ground state flip to the bare state $|3\rangle$ with positive imaginary component therefore the probability amplitude experience the exponential amplification which is stronger amplification in comparison to the negligible amplification into the probability amplitude of the the bare state $|2\rangle$ meanwhile the population in state the bare As clearly is shown in the Figure(2.9) the complete population transfer from the old ground state ($|1\rangle$) to the new ground state ($|3\rangle$). Therefore, by choosing the correct form of the parameters in the effective 2×2 Hamiltonian, we can expect complete population transfer in higher dimension.

2.7 DASA Vs traditional Shortcut to Adiabaticity

As discussed in the earlier section, complete population transfer through the common shortcut to adiabaticity approaches is accessible by using the extra field in order to cancel the effect of the existing non-adiabatic channels in the diabatic process. On the other hand, in our dynamical approach, the extra field has been used too. However, there exist three differences between DASA and typical non-Hermitian shortcut to adiabaticity. First of all, as a matter of the gain accumulated into the system, if we integrate the function of Equations.(2.17) it would be 13.27 for the two-level non-Hermitian LZ example, in the section 2.4 while, the total amount of gain accumulated through DASA, is equal to the gain in the first part of the dynamic. Meaningly ($-15 < t < -12$) the gain is equal to 0.01 and in the second part of the dynamics ($-12 < t < -11.358$) it is equal to the 3.99 , sums up to $0.009 * 3 + 3.99 * 0.642 \approx 2.588$. Secondly, the gain/loss profile used during the process might not be a simple function. For example, in the presented non-Hermitian STA the Lorentzian functional form of the gain profile depends on time and at $t = 0$ the gain needed to realize the population inversion

increase. Therefore, it would be challenging to create such a function. Finally, If we compare the population inversion time period in DASA and the STA, we will realize that DASA provides much faster complete transition.

2.8 Experimental Setups

Our approach (DASA) can be implemented in different electrical, optical and acoustical setup. In this section, we present two realizations of the dynamical approach to shortcut to adiabaticity. First, in the optical setup, where two waveguides coupled to each other and second, in the electronic circuits. In the former, as depicted in Figure(2.10), each waveguide has two segments with different index of refraction plays the role of the on-site potential of the Hamiltonian $\mathcal{H}_{2 \times 2}(t)$. in spite of the fact that in the system of the coupled waveguides, t will be replaced by z . In the first segment of Figure(2.10) when $z = (0, z_1)$, each of the gain (left) or loss (right) waveguide has index of refraction $n^{l(r)}(z) = n_1^{l(r)} - i\gamma_1^{l(r)}$ and $n^{l(r)}(z) = n_2^{l(r)} + i\gamma_2^{l(r)}$ while in the second segment between $z = (z_1, z_2)$ different set of parameters have been used. l, r represent left and right waveguide.

The bottom Figure2.10, also show the electronic platform to realize DASA where, LM356 voltage doubling amplifier provides gain while a variable resistance generate loss. It involves gain and loss waveguide. While the loss is usually generated by metal coating, the gain is created using optical or electrical pumping.

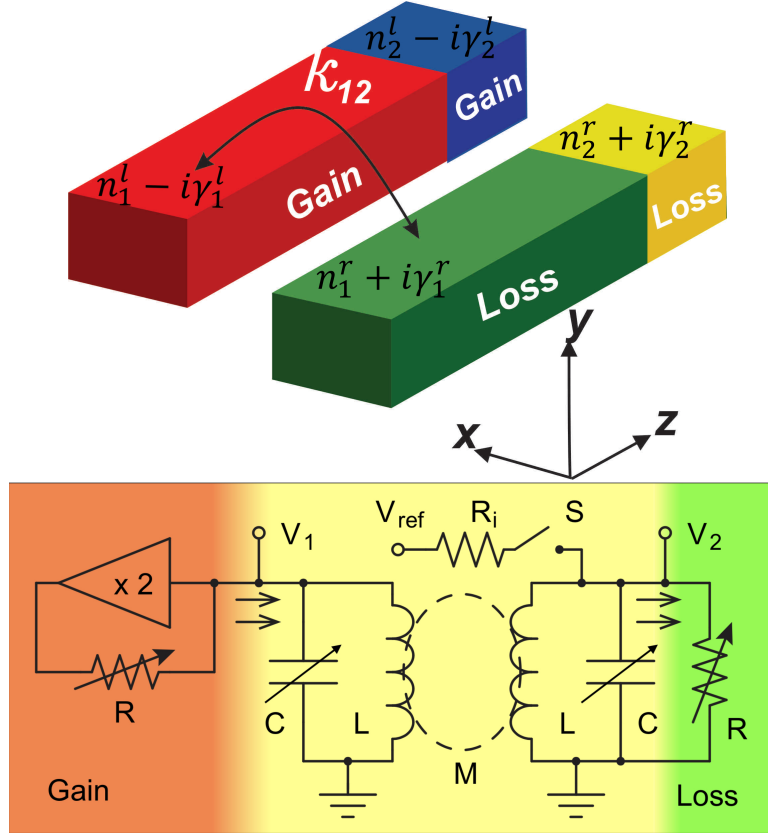


Figure 2.10: Upper figure, schematic of the proposed photonic structure to realize the dynamical approach to shortcut to adiabaticity. Our proposed structure composed of two waveguides. Each waveguide has two segments. The left waveguide in the first segment between $z = 0, z_1$ (indicated by the red color) has index of refraction $n_1^l - i\gamma_1^l$ while the right waveguide in the first segment has loss with refractive index $n_1^r - i\gamma_1^r$. In the second segment the left and right waveguides have refractive index $n_2^l + i\gamma_2^l$ and $n_2^r + i\gamma_2^r$ respectively. One can achieve complete population transfer in no time in terms of the electric fields if the values of $\gamma_{1,2}^l$ are chosen according to the g -functions in Equation.(2.25) and the real part of the refractive indexes are replaced by $\omega_{1,2}$. The bottom figure, Electronic implementation of dynamical approach to shortcut to adiabaticity. The coils are inductively coupled with V_1 and V_2 providing access to the system variables. The switch S asserts the initial condition. A resistor provides the damping (green side) while a negative resistance gain element (red side) is implemented by feedback from an LM356 voltage doubling amplifier. Current flows in the direction of the arrows proportional to the respective voltages V_1 and V_2 . Figures are taken from [71]

2.9 Summary

In this chapter, we study the adiabatic theorem. Although the adiabatic passage provides the promising result, it takes a long time to follow the necessary conditions of the adiabatic theorem. In practice arranging such a system without any interaction with the environment and being isolated is hard to realize. Alternatively, in order to prepare the desired quantum target state new approaches as shortcut to adiabaticity have been reviewed using the simple example of the two-level system. We showed that if one wants to follow the diabatic passage in the Hermitian system with the cost of increasing the coupling between the states we can reach the complete population transfer. Moreover, adding non-Hermiticity provides the possibility of having fast passage to population transfer while it enables us to bypass the strongly coupled states. After all, we introduce our new class of non-Hermitian Hamiltonian. We offer a dynamical approach as shortcut to adiabaticity. In our particular 2×2 proposed Hamiltonian, the specific form of the eigenvalues comes to our benefit in such a way that dynamically, the probability amplitude in the undesired eigenvalue experience decay or amplification while the other eigenstate keeps its probability amplitude constant. Finally, we have presented that our dynamical approach can be extended to the higher dimension system using the parameters of the proposed two-level Hamiltonian.

CHAPTER III

TOPOLOGICAL LOCALIZED STATE AT WILL

The concept of topologically protected state and their unique property to close the gap of the spectrum through the localization at the edge or interfaces of distinct systems is very important due to its robust characteristics against local perturbation. Therefore, topological state is considered as a promising property to investigate and implement in the experimental setup. Generally, in order to study and explore any kind of system, we can look and rely on the Lagrangian or Hamiltonian of the system to get all the necessary and sufficient information. In this thesis, we focus on the Hamiltonian considered as the Hermitian operator ensures the existence of a real spectrum for, E and describes the closed system which preserves the conservation of energy law. However, in reality, there exist some systems that have interaction with their environment. The behavior and dynamics of such an open system will be addressed through the Non-Hermitian Hamiltonian. Generally, the eigenvalues of the Non-Hermitian Hamiltonian are complex but in the special case when the Hamiltonian has particular PT -symmetry, under the specific condition it would have real spectrum unless it is spontaneously broken.

Currently, Topological properties are expanded to the non-Hermitian systems. Therefore, in this chapter, we will focus first of all, on review the previous studies in non-Hermitian realm, then we will introduce our new approach. Through this chapter we consider a two-level system and study the one-dimensional system expanded to the open Non-Hermitian chain of dimers depicted in Figure (3.1), consisting of two different sublattices A and B with the amplitudes ψ_n^A and φ_n^B in each of the sites respectively. The coupling factor in a dimer (intrapair) and out of it (interpair) denoted by k and c respectively, while the complex on-site potential denoted by γ

describes the amount of amplification or dissipation on each site. In the tight binding model, the time evolution of the field is governed by the Schrödinger:

$$\begin{aligned} i\partial_t \psi_n^A &= k\phi_n^B + c\phi_{n-1}^B - i\gamma\psi_n^A \\ i\partial_t \phi_n^B &= k\psi_n^A + c\psi_{n+1}^A + i\gamma\phi_n^B \end{aligned} \quad (3.1)$$

therefore, the associated Hamiltonian using the Bloch theorem is given by,

$$H(q) = (c \cos(q) + k)\sigma_x + c \sin(q)\sigma_y - i\gamma\sigma_z \quad (3.2)$$

where q is the Bloch wave number and $\sigma_i, i = 1, 2, 3$, are the Pauli matrices.

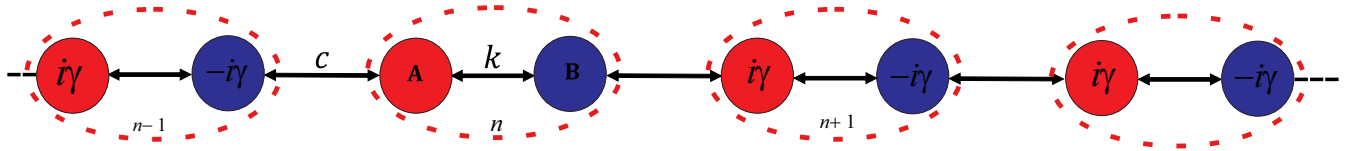


Figure 3.1: Sketch of Non-Hermitian chain of dimers structure. Two different sublattices distinguished by A represents the gain waveguide/resonator and B represents lossy waveguide/resonator, per unit cell, with $\pm i\gamma$ as the imaginary part of the on-site potential.

The Hamiltonian in Equation.(3.2) results in the dispersion relation

$$E(q) = \pm \sqrt{c^2 + k^2 - \gamma^2 + 2ck\cos q} \quad (3.3)$$

which in the absence of the complex part $\gamma = 0$ possess pure real band structure Figure (1.3).

3.1 Non-Hermitian PT Symmetric System

In mechanics besides the continuous symmetry operation obtained by applying successively infinitesimal operator, there are some discrete symmetry operators like, parity and time reversal. The parity or space inversion is the linear operator applied on the coordinate of the system such

that

$$P : \langle \alpha | P^\dagger x P | \alpha \rangle = -\langle \alpha | x | \alpha \rangle. \quad (3.4)$$

which simply means that the transformation changes the right-handed (RH) system to the left-handed (LH) or $P : \hat{x} \longrightarrow -\hat{x}$; it is also applied the same transformation on the momentum space like $\hat{p} \longrightarrow -\hat{p}$. On the other the operator called anti-linear if

$$A(c_1|\alpha\rangle + c_2|\beta\rangle) = c_1^*A|\alpha\rangle + c_2^*A|\beta\rangle \quad (3.5)$$

like the time-reversal operator, inverse time and momentum but not the space meaning $T : i \longrightarrow -i; \hat{x} \longrightarrow \hat{x}; \hat{p} \longrightarrow -\hat{p}$. In particular case there exist such a Hamiltonian that neither obey parity nor time-reversal symmetry separately, but instead respects the combined PT symmetry. The same as we said the Hamiltonian H commutes with the combined PT operator, i.e. $[PT, H] = 0$. As an example the Hamiltonian in Equation.(3.2) is the one that satisfy the commutation relation and remains unchanged under PT operator. The Hamiltonian in Equation.(3.2) have the complex potential $V(x) = i\gamma\sigma_z$ satisfies the following relation

$$V(x) = V^*(-x) \quad (3.6)$$

imposes the condition on the functional form of the potential that should be odd when it is imaginary. Although this class of Hamiltonian is considered to describe the system, with interaction to the environment, it also exhibit the real eigenvalues or energy spectrum as long as the non-Hermiticity parameter, γ , does not exceed a critical value $|k - c|$. More precisely, the system will remain in exact phase, otherwise phase transition occurs at the exceptional point where the Hamiltonian H is defective and does not have a complete basis of eigenvectors and the eigenvalues of the Hamiltonian H become degenerate. The PT symmetry of the Hamiltonian is spontaneously broken when the spectrum of the eigenvalues becomes complex. In particular the structure possess two phases, broken phase with complex spectrum and symmetric phase with pure real modes.

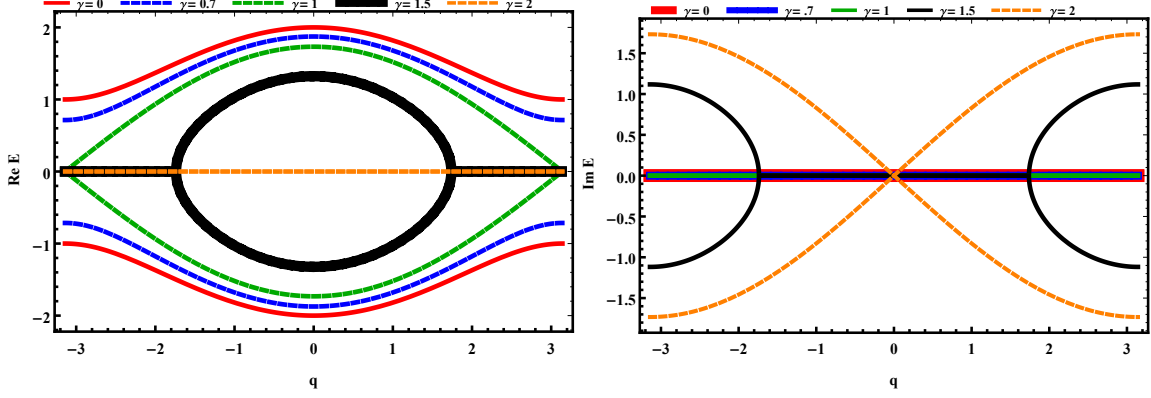


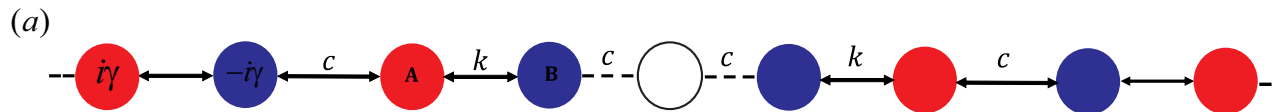
Figure 3.2: Sketch of dispersion relation of the complex SSH model. Left Figure, $\text{Re } E(q)$ and right figure dispersion $\text{Im } E(q)$ of the extended states for the biatomic lattice for various values of γ as the non-Hermitian part of the Hamiltonian and when the coupling $k = 0.5$ and $c = 1.5$. The dispersion relation are gapped when $\gamma < \gamma_c$ and the whole structure is in the exact phase of the PT system where the bands are totally real. The band gap closes at the phase transition point called exceptional point at $q = \pm\pi$. Then after, when the γ exceed the critical value.

As it is shown in the Figure (3.2), the non-Hermitian parameter γ plays an important role in the band structure as well as dynamics of the system. The non-Hermitian PT symmetric system faces phase transition in its eigenvalue spectrum from real to complex domain when γ deviate from the value $|k - c|$. In the Figure (3.2), the red solid line represents the upper and lower band structure when $\gamma = 0$ and the hopping parameters are antisymmetric while the dashed lines shows the spectrum for different values of γ . As it is depicted in the Figure (3.2), the gap between the two bands is closed when non-Hermiticity added to the system, but it is still totally real before the critical value while there is non-Hermitian parameter in the Hamiltonian.

3.2 Localized Mid-gap State in Non-Hermitian Lattice

The topological localized state is studied to the Non-Hermitian systems. The earlier investigation of topological characteristics on the extension of the SSH model to the Non-Hermitian system, starts with the observation of the mid-gap state with zero energy in the photonic lattice realized in the one dimensional photonic laser [73], where Schomerus claimed

there exists a defect state with localized characteristic at the interface of two topologically different configuration array of dimers Figure.(3.3 (a)). In such a structure, in the left semi infinite chain, the intrapair coupling is denoted by k considered as the strong bond between the sites, while the outer coupling interpair is denoted by c and considered as the weak bond. The second configuration is the right semi infinite chain in which, the sequence of the sites and coupling interchange. If we look at the structure more carefully the defect tunneling at the interface of two sides, is different from the tunneling at each edges of the structure for the odd number of sites. Therefore, we can interpret the whole lattice consist of two sides with different dimerization. Consequently, at the interface of these two distinct structures, a defect state emerges Figure.(3.3 a). The Hamiltonian of the Figure.(3.3) in particular case could represent the PT symmetric structure. Therefore, it would exhibit real spectrum as long as the γ does not exceed the critical point. Moreover, when σ_z vanishes, the Hamiltonian of Equation.(3.2) would represent the same characteristics of the Hermitian system with complete real eigenvalues. As a result, for the non-Hermitian Hamiltonian of such system in the unbroken phase quantization of the Berry phase or Zak phase in one dimension leads to the same result of the Hermitian Hamiltonian presented in the introduction. The difference between the localized state in the non-Hermitian lattice and its Hermitian counterpart is that while the energy of the Hermitian defect state pinned to zero, the defect state in the complex system, acquires non-zero imaginary part.



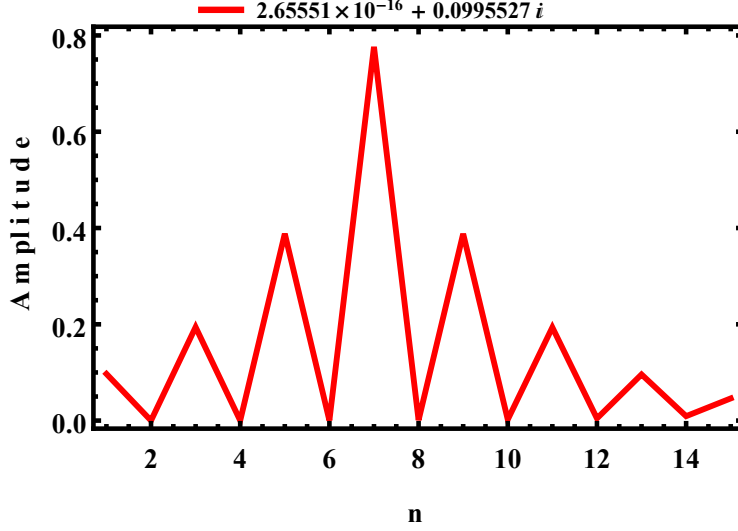


Figure 3.3: (a) Two coupled complex SSH chain with alternating bond k and c and alternating on-site potential $\pm i\gamma$ presenting two distinct topological configurations, result in having the defect state at the interface of two structures. (Bottom figure), As long as the on-site potential $\gamma < \gamma_c = |k - c|$, the exponentially localized state confined in the A sublattices when $k = 1$ and $c = 0.5$.

Schomerus showed that the Non-Hermitian system also can exhibit the topologically localized state, namely, The mid-gap state while, there still exist a gap in the band structure of both semi infinite chain. The mid-gap state also is protected against disorder in the coupling .

3.3 Topological invariant in the Non-Hermitian System

The topological phase of the closed system in one dimension is given by the Berry phase picked up by the eigenvectors, called Zak phase, when they sweep the Brillouin zone. The quantized Zak phase particularly named the winding number, determines the topological properties of the structure whether it is trivial without any edge state in the ordinary structures or non-trivial with the existence of an edge state acquires particular characteristics hidden from the environment. However, the calculation of the Berry phase differs for the non-Hermitian Hamiltonian, since the eigenvectors are no longer orthogonal and the corresponding eigenvalues are not real .

Therefore, generally the Berry phase becomes complex. Although, similar calculation is still

valid for the PT structures in their unbroken phase, the topological invariant are still not well-defined in the non-Hermitian systems. In general, we need to modify the Berry phase calculation in presence of non-Hermiticity. For the non-Hermitian PT symmetric Hamiltonian with biorthogonal pair of eigenvectors, the complex Berry phase is given by

$$\gamma_n = i \oint \langle L_n | \nabla_q | R_n \rangle \cdot dq \quad (3.7)$$

where the $\langle L_n |$ and the $| R_n \rangle$ are the left and right eigenvectors of the Hamiltonian, resulted to the continuous variation in the Berry phase.

3.4 Robust Localized Zero-Mode State Via Phase Transition in Non-Hermitian PT Symmetric Lattice

In this section, we will review an intriguing scenario to create zero-mode state while the periodicity in couplings is not broken. To this aim, the photonic lattice is again based on the non-Hermitian extension of the SSH model, consists of two coupled chains of dimers while they posses the PT characteristics, see Figure (3.1). Hence, there would be no topological defect state which breaks periodicity and all couplings posses the same topological order like their surroundings, localized state does not emerge. . We know that in the conventional scenario in Hermitian system and in the particular case of the Non-Hermitian Hamiltonian, when the topological nature of the coupling is the same as its surroundings, zero mode state becomes vanishing. However, according to Feng et al, it has been shown that Non-Hermitian phase transition in a parity-time PT symmetric lattice guarantees the existence of the protected zero mode state[25]. They showed that depending on the loss contrast in each site, three different possible phase can be found, while the transition between these phases does not alter the topological nature of the structure. In their formalism the Hamiltonian in the momentum space in Equation.(3.2) modified with the additional background loss term and the coupling k and c replaced by t_A and t_B respectively, which describes the PT symmetric system in the

following form

$$H(q) = -i\gamma_0 I + (t_B \cos(q) + t_A)\sigma_x + t_B \sin(q)\sigma_y + i\gamma\sigma_z \quad (3.8)$$

consequently, if we diagonalized the Hamiltonian, the energy dispersion reads as

$$E(q) = \epsilon_{\pm} + i\gamma_0 = \pm \sqrt{t_B^2 + t_A^2 - \gamma^2 + 2t_B t_A \cos q} \quad (3.9)$$

in which $2\gamma = \gamma_A - \gamma_B$ indicates the gain/loss contrast within one dimer. Based on the value of γ in Equation.(3.9), three different phases of unbroken PT , partially broken and completely broken phase with pure real, complex and totally imaginary dispersion energy are presumed. Consequently, variation of gain/loss leads to phase transition, though it does not change the topological nature of the system[25].

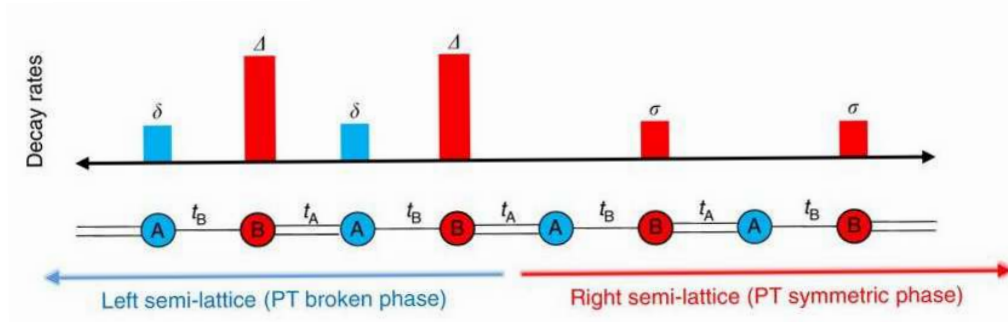


Figure 3.4: Schematic of an interface realized by two dissipative SSH semi-lattices with uniform coupling relation $t_A > t_B$ through the whole structure. Although the interface coupling has the same topological order as its neighbours, variation of gain/loss caused phase transition. Sites A have lower decay rates δ or 0 and sites B are associated with higher rates Δ or σ . Figure is taken from [25].

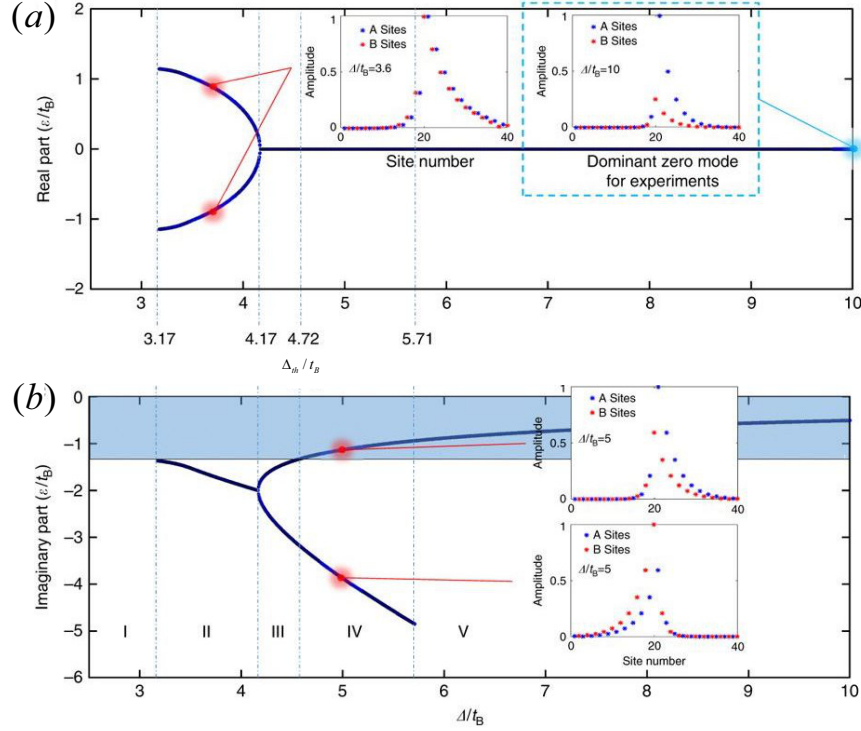


Figure 3.5: Energy diagram of the interface states for $t_A/t_B = 2.5$ and $\sigma = 2.5t_B$, and for the right semi-array in the unbroken PT phase (phase I: $\delta = 2.5t_B$). As $\frac{\Delta}{t_B}$ increases, five distinct regions can be defined: Region I, no interface state exist; Region II, there are two interface modes with opposite real part of energy; Region III, two zero-energy modes exist with different decay rates; Region IV, one of the two zero-energy modes becomes dominant in the system; Region V. The value of $\frac{\Delta}{t_B}$, separates regions III and IV is the threshold value $\frac{\Delta_{th}}{t_B}$ required to observe a dominant zero-energy mode in the dynamics. The insets show a few distributions of mode amplitudes of interface states at a few values of $\frac{\Delta}{t_B}$. Figure is taken from [25].

As it is shown in the Figure (3.4) and (3.5), the interface connected two semi-array whose energy spectrum are decoupled from each other in the real domain. Therefore, due to the lack of coupled state, the localized state with zero energy is generated at the interface. experimental realizations of such structure is conducted using an array of coupled waveguides where each waveguide represents a site (A or B) in the SSH model see Figure.(3.6a)

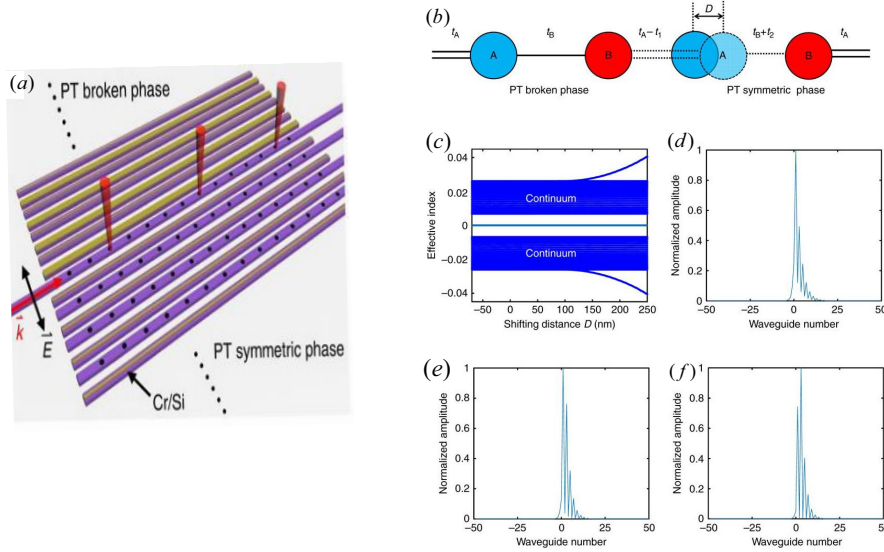


Figure 3.6: (a) The schematic of array of waveguides maintain zero-mode state at the interface of PT broken and un-broken phase of semi-lattices. (b) Schematic of the perturb structure where the interface waveguide is shifted by a distance D from its original place. Therefore the disorder applied to the interface coupling. (c) Evolution of eigen-spectrum with respect to the shift of the interface waveguide. The interface state robustly resides at zero energy apart from the extended states. (d-e) Intensity of the the localized state with zero-energy correspond to different shift at the interface waveguide. Figure is taken from [25].

3.5 Zero-Mode Protected State at Will in PT Symmetric Lattice

We reviewed two different approaches lead to emergence of the zero-mode energy state, either by transition in the topological nature of the structure or inducing the phase transition.

Generally, the localized state appear, if there exist any kind of defect which breaks periodicity in the structure. However, not necessarily all of them maintain zero energy. In this section, we would like to address the question "whether it is possible to observe the robust bound state in the periodic chain of dimers while the coupling of the defect state has the same topological order as its surrounding does?". To address this question, unlike previous investigations, we are interested to explore the existence and robustness of such edge state in non-Hermitian system where uniform pump configuration is realized just at the interface of two semi-infinite,

non-trivial chain of dimers. Consider a non-Hermitian (1D) chain of dimers like Figure(3.1) to be divided into two semi-infinite non-trivial arrays where $k = 0.5$ and $c = 1$. Suppose, the two arrays are connected to each other via an interface coupling namely, d . When the system is ordered $d = c$, in the both case of $\gamma = 0$ or $\gamma = |k - c|$, it is expected that all the sites are coupled to each other and construct the band structure of the system as shown in the Figure (3.7). Therefore, non of the modes are apart from the band.

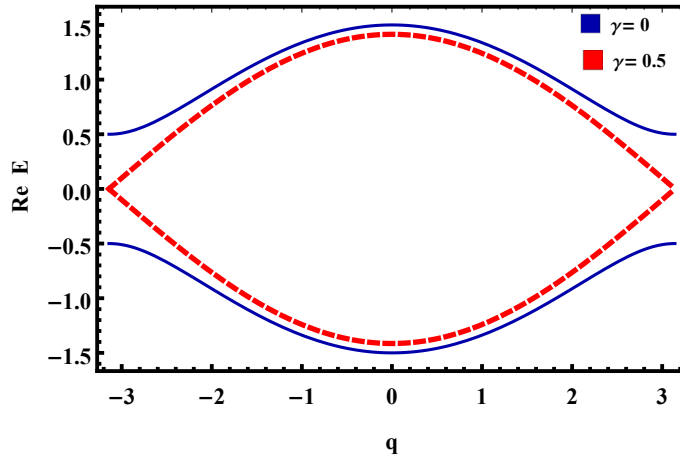


Figure 3.7: Sketch of dispersion, $\text{Re } E(q)$, of the extended states for the biatomic lattice where $\gamma = 0$ and the gap is open. On the other hand, $\gamma = 0.5$ reduced the effective coupling. Therefore, the gap is closed when $k = 0.5$ and $c = 1$.

On the other hand, when there is a defect in the coupling namely $d \neq c$, the localized state emerges. Now, lets see how the on-site potential comes into place. Equation.(3.3), clearly shows that addition of on-site potential shifted the eigenvalues of the Hamiltonian, meanwhile, it plays an important role to determine the phase of the structure. At the presence of non-Hermiticity in the structure, When the periodicity breaks in the lattice the corresponding mode to the confined state could be found either in the symmetric phase with the real energy or it could be in its broken phase where the mode becomes complex. Depending on the gain/loss, we have control over the phase of the eigenmode. By alternating the effective coupling between dimers, one can cause a decoupling mechanism while at the same time induce transition from localized state with real energy Figure(3.8 left plot), to bound state maintains zero-energy

Figure(3.8 right plot).

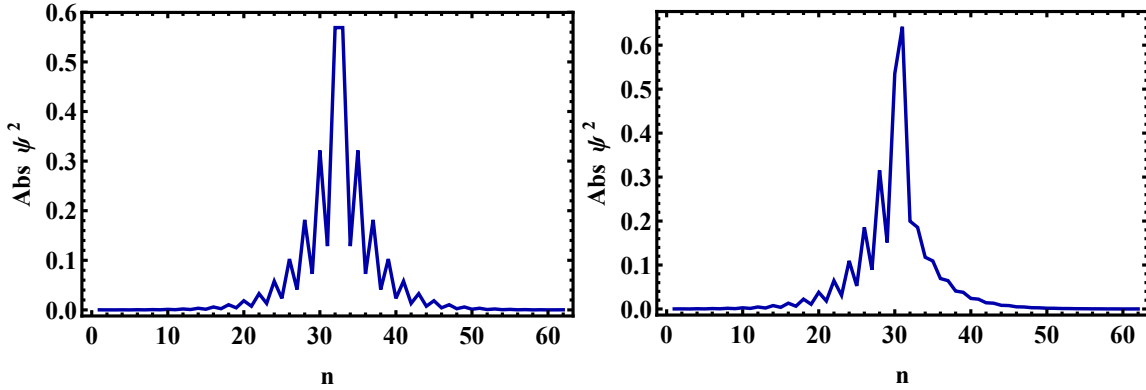


Figure 3.8: The mode amplitude of the localized state at the interface of two non-trivial structure. Left figure, when $\gamma = 0$ and localized state has real value eigenmode due to hermiticity of the structure. Right figure, when $\gamma = 0.041$ applied to the whole structure represents the PT symmetric lattice.

Motivated by this property and special characteristics provided by PT symmetric structures, we realize that not only we can keep the whole structure in the same topology, but also, in order to create zero energy state, there is no need to apply gain/loss through the whole structure.

Consider the case where the gain/loss is removed from all the sublattices except two of the sites in neighbor of the defect coupling namely $d = 0.04$. So, the pump configuration representing the PT symmetric structure, introduce the robust defect state with zero-energy while no phase transition occur between the two sides of the lattice. Figure (3.9) shows that while the non-Hermiticity increases in the Hamiltonian the phase of the eigenmodes incline toward its broken phase.

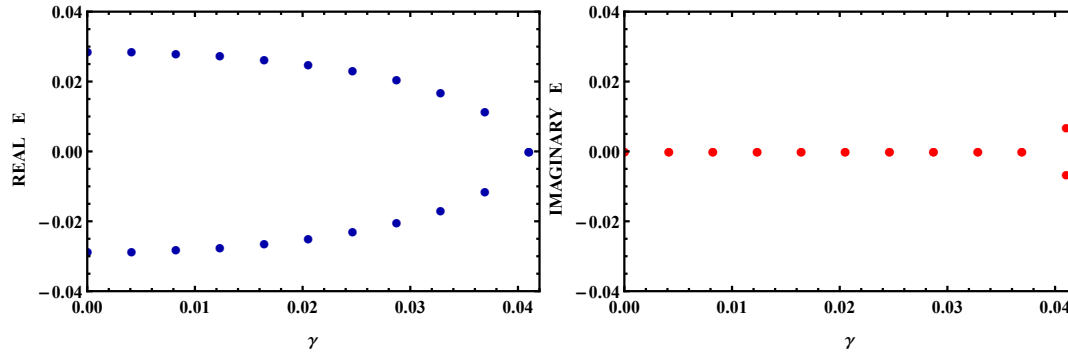


Figure 3.9: As the non-Hermiticity increases from $\gamma = 0$ toward the critical value $\gamma = 0.041$, the real part of the defect mode decreases while imaginary part grows, till the mode falls into its complete broken phase and energy pins to zero.

In addition we claim that the defect state with zero energy vanishes whenever the applied gain/loss deviates from the critical value. So, the value of γ plays an important role to make the decoupling mechanism. Our approach can be implemented in different experimental setups such as photonic crystals like coupled waveguide or resonators[74]. In the numerical calculation, the lattice composed a chain of dimmers $n=62$ with periodic coupling $c > k$. We terminate the bond with smaller coupling, therefore non trivial coupling or lack of dimerization at each side caused edge states. Next, we break the periodicity in the coupling by inserting a defect in the structure, it is good to mention that there is no restriction in the position of the defect coupling and we are free to choose the position of the defect. As mentioned earlier, entering defect in the structure caused localized state, then by increasing the value of gain/loss in the neighbor coupling not only the whole structure transit to the broken phase, but also by adjusting the pump we can shift the defect mode to zero. Therefor in this case we reach the localized state which has zero energy. Whereas in previous studies transition in the topological order of the structure or phase of system is needed for the emergence of a robust localized state, interestingly, uniform pump configuration makes it easier for us to choose the decoupled sites at will while we used less energy. To clarify the origin of the emergence of a bound state in the latest approach, compare bound states generated at will with zero-energy, left Figure(3.10, with

the localized state created in the Hermitian chain of dimers while the gain/loss applied on to the very first sublattice. As it is shown in the right Figure(3.10, the same amount of gain/loss profile caused the localized states looks alike which assure that the decoupled state in the middle of the two semi-infinite lattices appear as the result of effective decoupling mechanism of additional non-Hermitian part in the structure.

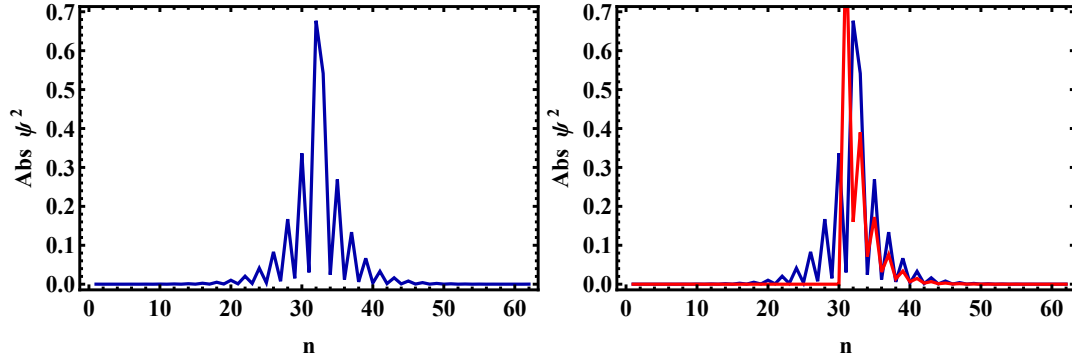


Figure 3.10: Topological localized state at the interface of two semi-infinite non-trivial lattices when $d = 0.4$ and $\gamma = 0.41$ applied to the edge sites, Left plot. Amplitude of the localized state (Blue state) emerges in the PT structure, compared with the decoupled state appear as non-Hermiticity applied to the edge sublattice, Red mode profile in the right plot.

3.6 Robustness of the zero mode

In previous section we show that by engineering the amount of gain/loss, we can control the energies of a defect state to become zero. Therefore, the modes transit from their symmetric phase to the broken phase meanwhile the mode becomes robust against disorder . We consider random perturbation in the platform of coupled resonators where one of the sub lattices is displaced from its position, consequently the inter couplings k changes through the whole structure. It has been shown that not only the field still remains localized, but also the energy of the localized state does not change and deviate from zero, regardless of the disorder strength, demonstrated in the Figure (3.11).

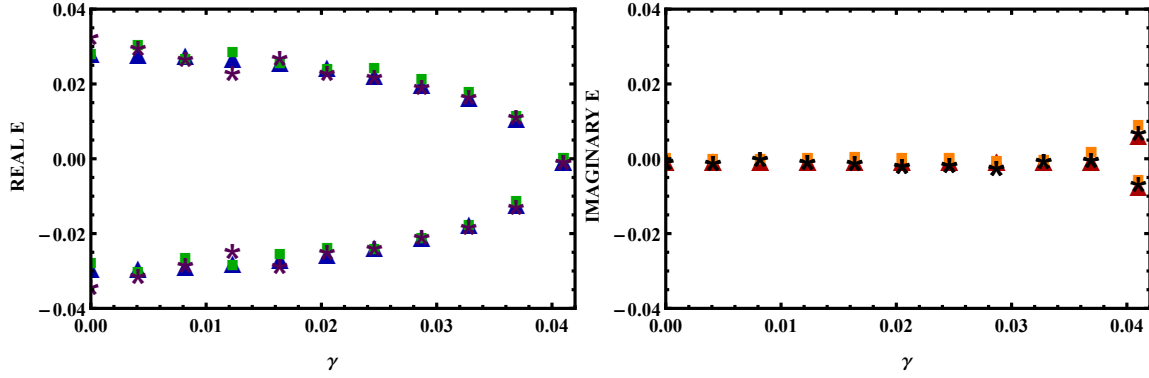


Figure 3.11: Robustness of the bound state mode at the presence of disorder with different strength. The plot shows that the defect mode when it falls into its broken phase, still pines to zero and is protected against local change applied to the structure.

3.7 Summary

In this chapter, we deal with topological characteristics of the non-Hermitian system. First part of the chapter dedicated to reviewing the previous investigation on the one dimensional expansion of the SSH model to the complex domain. We review the mid-gap state which is the 1D arrays of dimers with two different topological configurations coupled to each other. As the topological invariant of the left and right structure are distinct at the interface an exponentially localized state emerges. Next, we reviewed a different investigation on robust localized state where in a non-Hermitian PT -symmetric structure, the ununiform pump configuration leads to the phase transition in the structure. Therefore, in the absence of coupling in the real part of the eigenvalues for two phases of the bands, the robust localized state observed. In the last part of the chapter, we introduce our new mechanism leads to creation of the robust localized state in the non-Hermitian system follows the PT -symmetric structure characteristics. In our one dimension lattice, we introduce a defect while two sides of the defect coupling found in the same configuration of topology. Consequently, not only we can keep the structure in the same phase but also the robust localized state observed just by the uniform pump. Our approach provides a flexible protocol in which at will, we are able to create the localized state by putting less amount of gain and loss into the system.

BIBLIOGRAPHY

- [1] M. V. Berry, “Quantal phase factors accompanying adiabatic changes,” *Proc. R. Soc. Lond. A* 392 (1984) 45–57
- [2] D. J. Griffiths, Introduction to quantum mechanics, “Parity Anomaly”, *Phys. Rev. Lett.* 61,(2015).
- [3] M. Born and V. Z. Fock, *Eur. Phys. J. A* 51, 165 (1928), doi:10.1007/BF01343193
- [4] A. Messiah, “Quantum mechanics”, Dover Publications, New York (1999).
- [5] A.C. Aguiar-Pinto, M.C. Nemes, J.G. Peixoto de Faria, and M.T. Thomaz, “Comment on the adiabatic condition,” *Am. J. Phys.* 68 (2000) 955–958, quant-ph/9912030
- [6] F. D. M. Haldane, Model for a Quantum Hall Effect without Landau Levels: Condensed-Matter Realization of the “Parity Anomaly”, *Phys. Rev. Lett.* 61,(2015).
- [7] A. Y. Kitaev, Fault-Tolerant Quantum Computation by Anyons, *Ann. Phys. (Amsterdam)* 303, 2 (2003).
- [8] C. Nayak, S. H. Simon, A. Stern, M. Freedman, and S. D. Sarma, Non-Abelian Anyons and Topological Quantum Computation, *Rev. Mod. Phys.* 80, 1083 (2008).
- [9] J. Alicea, Y. Oreg, G. Refael, F. von Oppen, and M. P. A. Fisher, Non-Abelian Statistics and Topological Quantum Information Processing in 1d Wire Networks, *Nat. Phys.* 7, 412 (2011).
- [10] R. Barends, J. Kelly, A. Megrant, A. Veitia, D. Sank, E. Jeffrey, T. C. White, J. Mutus, A. G. Fowler, B. Campbell, Y. Chen, Z. Chen, B. Chiaro, A. Dunsworth, C. Neill, P. O’Malley, P. Roushan, A. Vainsencher, J. Wenner, A. N. Korotkov, A. N. Cleland, and J. M. Martinis, Superconducting Quantum Circuits at the Surface Code Threshold for Fault Tolerance, *Nature (London)* 508, 500 (2014).
- [11] F. D. M. Haldane and S. Raghu, Possible Realization of Directional Optical Waveguides in Photonic Crystals with Broken Time-Reversal Symmetry, *Phys. Rev. Lett.* 100, 013904 (2008).
- [12] M. Hafezi, E. A. Demler, M. D. Lukin, and J. M. Taylor, Robust Optical Delay Lines with Topological Protection, *Nat. Phys.* 7, 907 (2011).
- [13] K. Fang, Z. Yu, and S. Fan, Realizing Effective Magnetic Field for Photons by Controlling the Phase of Dynamic Modulation, *Nat. Photonics* 6, 782 (2012).

- [14] A. B. Khanikaev, S. H. Mousavi, W.-K. Tse, M. Kargarian, A. H. MacDonald, and G. Shvets, Photonic Topological Insulators, *Nat. Mater.* 12, 233 (2013).
- [15] I. Carusotto and C. Ciuti, Quantum Fluids of Light, *Rev. Mod. Phys.* 85, 299 (2013).
- [16] M. Hafezi, S. Mittal, J. Fan, A. Migdall, and J. M. Taylor, Imaging Topological Edge States in Silicon Photonics, *Nat. Photonics* 7, 1001 (2013).
- [17] M. C. Rechtsman, J. M. Zeuner, Y. Plotnik, Y. Lumer, D. Podolsky, F. Dreisow, S. Nolte, M. Segev, and A. Szameit, Photonic Floquet Topological Insulators, *Nature (London)* 496, 196 (2013).
- [18] L. Lu, J. D. Joannopoulos, and M. Soljačić, Topological Photonics, *Nat. Photonics* 8, 821 (2014).
- [19] T. Karzig, C.-E. Bardyn, N. H. Lindner, and G. Refael, Topological Polaritons, *Phys. Rev. X* 5, 031001 (2015).
- [20] T. Ozawa, H. M. Price, A. Amo, N. Goldman, M. Hafezi, L. Lu, M. Rechtsman, D. Schuster, J. Simon, O. Zilberberg, and I. Carusotto, Topological Photonics, arXiv:1802.04173.
- [21] w. p. su, j. r. schrieffer, and a. j. heeger, *phys. rev. lett.* 42, 1698 (1979).
- [22] B. Perez-Gonzalez, M. Bello, A. Gomez-Leon and G. Platero, arXiv:1802.03973 (2018).
- [23] Maria Maffei, Alexandre Dauphin, Filippo Cardano, Maciej Lewenstein, and Pietro Massignan, <https://arxiv.org/pdf/1708.02778> (2018).
- [24] J. M. Zeuner, M. C. Rechtsman, Y. Plotnik, Y. Lumer, S. Nolte, M. S. Rudner, M. Segev, and A. Szameit, Observation of a Topological Transition in the Bulk of a Non-Hermitian System, *Phys. Rev. Lett.* 115, 040402 (2015).
- [25] J. M. Pan, Han Z, Pei Miao, S. Longhi and L. Feng, Photonic zero mode in a non-Hermitian photonic lattice, *Nature Communications* volume 9, 1308 (2018).
- [26] C. Yuce, Topological phase in a non-Hermitian PT symmetric system, *Physics Letters A* 379 (2015).
- [27] Ramy El-Ganainy, Konstantinos G. Makris, Mercedeh Khajavikhan, Ziad H. Musslimani, Stefan Rotter and Demetrios N. Christodoulides, Non-Hermitian physics and PT symmetry, *Nature Physics* volume 14, pages 11–19 (2018).
- [28] N. V. Vitanov, A. A. Rangelov, B. W. Shore, and K. Bergmann, *Rev. Mod. Phys.* 89, 015006 (2017), doi:10.1103/RevModPhys.89.015006.
- [29] Nikolay V. Vitanov, Thomas Halfmann, Bruce W. Shore, and Klaas Bergmann, *Annual Review of Physical Chemistry*, 52, 1, 763-809 (2001), doi:10.1146/annurev.physchem.52.1.763.

- [30] K. Eckert, M. Lewenstein, R. Corbalan, G. Birkl, W. Ertmer, and J. Mompart, *Phys. Rev. A* 70, 023606 (2004).
- [31] A. D. Greentree, J. H. Cole, A. R. Hamilton, and L. C. L. Hollenberg, *Phys. Rev. B* 70, 235317 (2004).
- [32] L. C. L. Hollenberg, A. D. Greentree, A. G. Fowler, and C. J. Wellard, *ibid.* 74, 045311 (2006).
- [33] K. Eckert, J. Mompart, R. Corbalan, M. Lewenstein, and G. Birkl, *Opt. Commun.* 264, 264 (2006).
- [34] J. E. Avron, R. Seiler, and L. G. Yaffe, *Commun. Math. Phys.* 110, 33 (1987).
- [35] P. Ehrenfest, “Adiabatische Invarianten und Quantentheorie,” *Ann. d. Phys.* 51 (1916) 327.
- [36] M. Born and V. Fock, “Beweis des Adiabatenatzes,” *Z. Phys.* 51 (1928) 165–180.
- [37] Martin Greiter, Frank Wilczek, *Nuclear Physics B*, 370, 577 (1992), doi:10.1016/0550-3213(92)90424-A.
- [38] G. E. Santoro and E. Tosatti, *J. Phys. A: Math. Gen.* 39, R393 (2006).
- [39] A. Das and B. K. Chakrabarti, *Rev. Mod. Phys.* 80, 1061 (2008).
- [40] M. W. Johnson, M. H. S. Amin, S. Gildert, T. Lanting, F. Hamze, N. Dickson, R. Harris, A. J. Berkley, J. Johansson, P. Bunyk, E. M. Chapple, C. Enderud, J. P. Hilton, K. Karimi, E. Ladizinsky, N. Ladizinsky, T. Oh, I. Perminov, C. Rich, M. C. Thom, E. Tolkacheva, C. J. S. Truncik, S. Uchaikin, J. Wang, B. Wilson, and G. Rose, *Nature (London)* 473, 194 (2012).
- [41] R. Babbush, P. J. Love, and A. Aspuru-Guzik, *Sci. Rep.* 4, 6603 (2014).
- [42] N. V. Vitanov and K.-A. Suominen, *Phys. Rev. A* 59, 4580 (1999).
- [43] N. V. Vitanov, L. P. Yatsenko, and K. Bergmann, *Phys. Rev. A* 68, 043401 (2003).
- [44] B. T. Torosov, S. Guerin, and N. V. Vitanov, *Phys. Rev. Lett.* 106, 233001 (2011).
- [45] M. M. T. Loy, *Phys. Rev. Lett.* 32, 814 (1974); 36, 1454 (1976); 41, 473 (1978); D. Grischkowsky and M. M. T. Loy, *Phys. Rev. A* 12, 1117 (1975); D. Grischkowsky, *ibid.* 14, 802 (1976).
- [46] N. V. Vitanov et al., *Annu. Rev. Phys. Chem.* 52, 763 (2001).
- [47] S. Guerin, S. Thomas, and H. R. Jauslin, *Phys. Rev. A* 65, 023409 (2002); G. Dridi, S. Guerin, V. Hakobyan, H. R. Jauslin, and H. Eleuch, *Phys. Rev. A* 80, 043408 (2009).
- [48] Demirplak M and Rice S A 2003 *J. Phys. Chem. A* 107 9937.
- [49] Demirplak M and Rice S A 2005 *J. Phys. Chem. B* 109 6838.

- [50] Demirplak M and Rice S A 2008 J. Chem. Phys. 129 154111.
- [51] Berry M V 2009 Journal of Physics A: Mathematical and Theoretical 42 365303.
- [52] Schaff J F, Song X L, Vignolo P and Labeyrie G 2010 Phys. Rev. A 82(3) 033430 URL <https://link.aps.org/doi/10.1103/PhysRevA.82.033430>.
- [53] Schaff J F, Song X L, Capuzzi P, Vignolo P and Labeyrie G 2011 EPL (Europhysics Letters) 93 23001 URL <http://stacks.iop.org/0295-5075/93/i=2/a=23001>.
- [54] Wang T, Zhang Z, Xiang L, Jia Z, Duan P, Cai W, Gong Z, Zong Z, Wu M, Wu J, Sun L, Yin Y and Guo G 2018 New Journal of Physics 20 065003 URL <https://doi.org/10.1088>
- [55] Deng J, Wang Q h, Liu Z, Hanggi P and Gong J 2013 Phys. Rev. E 88(6) 062122 URL <https://link.aps.org/doi/10.1103/PhysRevE.88.062122>.
- [56] del Campo A, Goold J and Paternostro M 2014 Sci. Rep. 4.
- [57] Tu Z C 2014 Phys. Rev. E 89(5) 052148.
- [58] Beau M, Jaramillo J and del Campo A 2016 Entropy 18 168 URL <http://www.mdpi.com/1099-4300/18/5/168> .
- [59] Chotorlishvili L, Azimi M, Stagracyński S, Toklikishvili Z, Schuler M and Berakdar J 2016 Phys. Rev. E 94(3) 032116.
- [60] Torrontegui E, Dawkins S T, Gb M and Singer K 2018 New Journal of Physics 20 105001.
- [61] C.M. Bender, D.C. Brody, H.F. Jones, and B.K. Meister, Phys. Rev. Lett. 98, 040403 (2007); R. Uzdin, U. Gunther, S. Rahav, and N. Moiseyev, J. Phys. A: Math. Theor. 45, 415304 (2012).
- [62] Landau L D and Lifshitz E M 2003 Quantum mechanics: non-relativistic theory 3rd ed (Butterworth-Heinemann).
- [63] Zener C 1932 Proc. Royal Soc. London A 137 696–702.
- [64] Boyan T. Torosov,* Giuseppe Della Valle, and Stefano Longhi. PHYSICAL REVIEW A 87, 052502 (2013).
- [65] B. T. Torosov, G. Della Valle, and S. Longhi,, Phys. Rev. A 87, 052502, (2013).
- [66] R. El-Ganainy, K.G. Makris, and D.N. Christodoulides, Phys. Rev. A 86, 033813 (2012).
- [67] A. Guo, G. J. Salamo, D. Duchesne, R. Morandotti, M. Volatier-Ravat, V. Aimez, G. A. Siviloglou, and D. N. Christodoulides, Phys. Rev. Lett. 103, 093902 (2009).
- [68] B. Peng, Ş. K. Özdemir, F. Lei, F. Monifi, M. Gianfreda, G. L. Long, S. Fan, F. Nori, C. M. Bender, and L. Yang, Nat. Phys. 10, 394 (2014).
- [69] J. Sheng, M. A. Miri, D. N. Christodoulides, and M. Xiao, Phys. Rev. A 88, 041803 (2013).

- [70] P. Peng, W. Cao, C. Shen, W. Qu, J. Wen, L. Jiang, and Y. Xiao, *Nat. Phys.* 12, 1139 (2016).
- [71] F Mostafavi, L Yuan, H Ramezani, *Physical review letters* 122 (5), 050404(2019).
- [72] Rahman Sharaf, Mojgan Dehghani, Hamidreza Ramezani, *Review A* , 97,(1), 013854 (2018).
- [73] H. Schomerus, *Opt. Lett.* 38, 1912 (2013).
- [74] Ling Lu, John D. Joannopoulos and Marin Soljačić, *Topological photonics*, *Nature Photonics* volume 8, pages 821–829 (2014).

BIOGRAPHICAL SKETCH

Fatemeh Mostafavi is an international student at The University of Texas Rio Grande Valley. she grew up in Tehran, Iran. After finishing her study in Iran . She moved to the USA, to continue her education at the graduate level. She joined the Physics program in Fall 2017 and earned a Master of Science degree with focus on non-Hermitian systems in August 2019.

During the master education, Fatemeh participated in research on non-Hermitian quantum and classical systems. She worked on different projects under supervision of Dr. Hamidreza Ramezani. The experiences through her education at physics department, provides her with valuable insight into the adiabatic theorem and population transfer, as well as topological systems and beyond.

The result of the present thesis was published Phys.Rev.Lett. Fatemeh also, is a member of American Physical Society. she presented her result at the APS March meeting, COS annual conference, and SACNAS conference. Participating in different conferences not only provides her a platform to introduce her research but also presents the opportunity to incite conversation with experienced researchers and herself that would be indispensable to her graduate study. In the short term, she looks forward to beginning Ph.D at different school to gain more knowledge and obtain more theoretical and practical experience in the field.

Email : fatemeh.mostafavikhatam01@utrgv.edu